

**COLLECTIVE TREATMENT OF THE PAIRING HAMILTONIAN****(I). Formulation of the model**D. R. BÈS, R. A. BROGLIA<sup>†</sup> and R. P. J. PERAZZO*University of Minnesota, Minneapolis, Minnesota 55455*<sup>††</sup>

and

K. KUMAR

*Oak Ridge National Laboratory, Oak Ridge, Tennessee*<sup>††</sup>

Received 1 September 1969

**Abstract:** We develop a treatment of the pairing force problem in terms of two collective variables: the intrinsic deformation  $\alpha$  and the gauge angle  $\phi$ . The comparison between the results obtained solving the corresponding quantum mechanical Hamiltonian and those obtained by an exact diagonalization shows the adequacy of the present approach.

**1. Introduction**

The interaction of the valence nucleons via a pairing force with constant matrix elements accounts for the energy gap in the excitation spectrum of even nuclei, the mass difference between even and odd nuclei, the value of the rotational moment of inertia and the enhancement of ground to ground state transitions in the process involving the transfer of two particles<sup>1</sup>). The existence of such a type of residual force in nuclei was first proposed by Bohr, Mottelson and Pines<sup>2</sup>). Its treatment is very much simplified by making the approximation of a superconducting field<sup>3,4</sup>). The corresponding violation of a symmetry which is present in the original Hamiltonian (the conservation of the number of particles) implies the existence of superconducting bands (for instance, the set of ground states of neighbouring even nuclei). The matrix elements of two-body transfer processes are very much enhanced between members of the same superconducting band and, indeed, these processes play the same rôle as the Coulomb excitation in rotational bands.

The existence of a vibrational degree of freedom associated with the pairing force, namely, the pairing vibration has been suggested<sup>5</sup>). The microscopic description of this mode has been made within the random-phase approximation, both for superfluids and normal systems<sup>6</sup>). The corresponding phonon carries  $J = 0$ ,  $\pi = +$ ,  $\sigma = 0$ ,  $\tau = 1$  and  $\alpha = \pm 2$ , where  $J$  is the angular momentum,  $\pi$  the parity,  $\sigma$  the spin,  $\tau$  the isospin and  $\alpha$  the baryon quantum number, respectively. Again, the specific experimental tools for checking the properties of these collective states are the two-body transfer reactions. Although there are regions of the periodic

<sup>†</sup> On leave from the Niels Bohr Institute, University of Copenhagen, Denmark.

<sup>††</sup> Work supported in part by the U. S. Atomic Energy Commission under Contract No. AT(11-1) 1764.

table which display the basic pattern predicted by the model <sup>7)</sup>, significant departures from harmonicity are found. Attempts to correct for these effects by means of a boson expansion have been made <sup>8)</sup>.

The aim of the present paper is to develop a macroscopic model of the collective degree of freedom associated with the pairing force which would include the anharmonic terms of the motion within the adiabatic approximation. The variables of the model are the gap parameter and the gauge angle <sup>9,10)</sup> which is the canonically conjugate variable to the number of particles operator. Thus, the model provides a unified description of systems displaying permanent superfluid distortions and normal systems. In particular, it allows one to follow the onset of stable superconducting distortions starting from closed shell normal nuclei.

In ref. <sup>18)</sup> (see appendix) the collective variables mentioned above are defined in terms of a boson expansion, and some properties of the potential energy surface are discussed in connection with two-nucleon transfer data.

In the present paper the model is presented and applied to the case of a system of particles moving in a set of symmetric single-particle levels with energy  $e_v = \nu e$  ( $\nu = \pm 1, \pm 2, \pm 3, \dots$ ). The numerical solution as well as the adiabatic approximation is checked by comparing the energies and matrix elements of the two-body transfer operator against the exact solution of the two-level model <sup>11)</sup>.

All the ideas and magnitudes presented here have their analogous counterpart in the macroscopic description of the quadrupole degree of freedom as formulated by Bohr <sup>12)</sup> and solved numerically by Baranger and Kumar <sup>13)</sup>.

In the present case of the pairing between identical particles, we have the advantage over the quadrupole case that the problem is much simpler (two collective variables instead of five, abelian instead of vector magnitudes, etc.). Moreover, because the exact treatment of the pairing force may be done in cases involving high degeneracies, we have the very infrequent possibility of comparing our results with exact ones in a meaningful way from the point of view of the theory of collective motion.

In future papers we intend to treat more realistic cases and to introduce the isospin degree of freedom.

## 2. The pairing collective coordinates

We obtain the collective variables associated with the pairing mode using as a guidance, the model of rotations and vibrations in a system undergoing quadrupole deformations.

Many properties of nuclei may be understood in terms of the shell model and an average quadrupole single-particle field. This field is easily obtained if we assume that an important component of the effective two-body Hamiltonian is represented by the quadrupole interaction

$$H_Q = -\frac{1}{2}\chi \sum_{\mu} Q_{\mu} Q_{\mu}^{\dagger}, \quad (2.1)$$

where

$$Q_\mu = \sum_{\nu, \nu'} m_{\nu, \nu'}^{(\mu)} c_\nu^\dagger c_{\nu'},$$

$$m_{\nu, \nu'}^{(\mu)} = \langle \nu | r^2 Y_{2\mu}(\theta, \phi) | \nu' \rangle, \quad (2.2)$$

and  $c_\nu^\dagger$  ( $c_\nu$ ) are the particle creation (annihilation) operators. Then, the average field due to other particles acting through  $H_Q$  on a particular nucleon represents the deformed field

$$V_Q = - \sum_\mu \kappa_\mu Q_\mu, \quad (2.3)$$

where  $\kappa_\mu^* = (-)^{\mu} \kappa_{-\mu}$  in order that  $V_Q$  be hermitian.

The determinantal eigenfunctions  $\psi(\kappa)$  of the many-body independent particle Hamiltonian

$$H'_Q(\kappa) = H_{\text{sph}} + V_Q, \quad (2.4)$$

are parametrized by the five (real) constants  $\kappa_\mu$  which determine the shape of the potential. Use is made of the notation  $\kappa \equiv (\kappa_\mu)$ . In eq. (2.4),  $H_{\text{sph}}$  represents a single-particle Hamiltonian with spherical symmetry. It is also convenient to define the related variables  $q_\mu$  as the expectation values

$$q_\mu = \langle \psi(\kappa) | Q_\mu^\dagger | \psi(\kappa) \rangle. \quad (2.5)$$

The parameters  $q_\mu$  measure the quadrupole deformation of the wave function. They can be much larger than the single-particle estimates provided by the spherical shell model. At equilibrium, it can be shown that

$$\chi q_\mu = \kappa_\mu. \quad (2.6)$$

We may expect a very simple type of motion in which the values of the parameters  $q_\mu$  (or  $\kappa_\mu$ ) change slowly with time, while the internal single-particle field follows adiabatically and thus holds the particles in almost the same state of intrinsic motion.

Instead of parametrizing the quadrupole distortion by the five parameters  $q_\mu$  we may specify the deformations in an intrinsic frame and use, as additional variables, the orientation of this particular frame. The intrinsic system of reference is oriented in such a way that only two independent deformation parameters are different from zero. It is customary to choose

$$q'_1 = q_{-1} = q'_2 - q'_{-2} = 0, \quad (2.7)$$

$$q'_0 = \frac{3}{20\pi} AR^2 \beta \cos \gamma,$$

$$q'_2 = \frac{3}{20\pi} AR^2 \frac{1}{\sqrt{2}} \beta \sin \gamma, \quad (2.8)$$

where  $A$  is the number of particles and  $R$  the nuclear radius. The parameter  $\beta$  is the (invariant with respect to rotations) quantity measuring the deformation,

$$\beta = \frac{20\pi}{3AR^2} \left[ \sum_{\mu} q_{\mu}^* q_{\mu} \right]^{\dagger} = \frac{20\pi}{3AR^2} \left[ \sum_{\mu} q'_{\mu}{}^* q'_{\mu} \right]^{\dagger},$$

while  $\gamma$  measures departures from axial symmetry. The real quantities  $q'_0, q'_2$  (or  $\beta, \gamma$ ) are referred to as the intrinsic collective coordinates. The angular collective coordinates are the Euler angles  $\omega \equiv (\phi, \theta, \varphi)$  that are defined by the conditions (2.7) and the transformation

$$q'_{\mu} = \sum_{\nu} q_{\nu} D_{\nu\mu}^2(\omega). \quad (2.9)$$

The Hamiltonian describing the dynamics of the quadrupole degree of freedom in terms of these variables was given by Bohr <sup>12</sup>). The detailed functional dependence of the mass parameters associated with this collective motion can be determined through a microscopic model of the system. Quite generally, the kinetic energy term does not contain cross derivatives in the intrinsic and angular variables. However, the separation between  $\beta, \gamma$  and  $\omega$  is not complete because the moments of inertia, (i.e. the mass parameter in the terms including derivatives with respect to  $\omega$ ) depend on  $\beta$  and  $\gamma$ . Nevertheless, it is convenient to write the wave function in terms of the rotation matrices.

$$\Psi_{n, n', I, M}(\beta, \gamma, \omega) = \left( \frac{2I+1}{8\pi^2} \right)^{\dagger} \sum_K \varphi_{K, I, n, n'}(\beta, \gamma) D_{MK}^I(\omega) \quad (2.10)$$

where  $n, n'$  are quantum numbers associated with the  $\beta, \gamma$  degrees of freedom. The separation of variables is achieved for instance, for axially symmetric rigidly deformed systems. In this case  $K$  becomes a good quantum number and consequently the sum in eq. (2.10) disappears.

While the lowest excitations of strongly deformed nuclei correspond to rotations with  $\gamma = 0$  and fixed values of  $\beta$ , collective states at somewhat higher energies are generated by vibrations of the system around the equilibrium shape ( $\beta$  and  $\gamma$  degrees of freedom). The system is always close to the equilibrium deformation given by (2.6).

In approximately spherical nuclei, the energies associated with the five collective degrees of freedom are about equal and a phonon-like spectrum does appear.

Let us now consider the pairing degree of freedom. The pairing interaction with constant matrix elements may be written in the form

$$H_p = -GPP^{\dagger}, \quad (2.1')$$

where

$$P = \sum_{\nu>0} c_{\nu}^{\dagger} c_{\nu}^{\dagger}, \quad (2.2')$$

and  $c_v^\dagger$  creates the single-particle time-reversed state of  $c_v^\dagger$ . The Hamiltonian  $H_p$  may be solved in the field approximation. Thus, we replace  $H_p$  by a generalized "single-particle" potential

$$V_p = -(\Delta_2 P + \Delta_{-2} P^\dagger), \quad (2.3')$$

where  $\Delta_2 = \Delta_{-2}^*$  in order that  $V_p$  be hermitian.

The many-particle eigenfunctions  $\psi(\Delta)$  of the independent-fermion Hamiltonian,

$$H'_p(\Delta) = H_{s.p.} + V_p, \quad (2.4')$$

are parameterized by the two real components of the complex numbers which determine the shape of the potential. The notation  $\Delta \equiv (\Delta_2, \Delta_{-2})$  is used. Here  $H_{s.p.}$  is a many-body independent-particle Hamiltonian. It is also useful to define the parameters  $\alpha_{\pm 2}$  measuring the deformation of the wave function,

$$\alpha_\mu = \langle \psi(\Delta) | P(\mu) | \psi(\Delta) \rangle, \quad (2.5')$$

$$\mu = \pm 2, \quad \text{where } P(2) = P \text{ and } P(-2) = P^\dagger.$$

At equilibrium, it can also be shown that

$$\Delta_\mu = G\alpha_\mu. \quad (2.6')$$

The non-zero expectation value of  $P(\mu)$  implies that the states  $\psi(\Delta)$  do not have a definite number of particles. This feature is analogous<sup>†</sup> to the fact that the quantity defined in eq. (2.5) may be much greater than the shell-model estimate, as a consequence of the use of a deformed single-particle potential which does not conserve angular momentum.

Also in the pairing case, we can expect a slow type of motion in which the complex parameters  $\alpha_\mu$  ( $\Delta_\mu$ ) change with time, while the internal single-fermion field  $H'_p$  follows adiabatically.

Instead of parametrizing the pairing deformation by the  $\alpha_\mu$  parameters, we may introduce a transformation to an intrinsic system characterized by the fact that the deformation is described by only one real parameter<sup>††</sup>. In the quadrupole case, the transformation from the laboratory system to the intrinsic system is generated by the unitary transformation

$$R(\theta_m) = e^{-iI_m \theta_m}. \quad (2.11)$$

On the other hand, we have already remarked that in connection with the pairing case the number of particles plays an analogous role to the angular momentum

<sup>†</sup> There is in this sense a small difference between the quadrupole and the pairing case. The quadrupole operator may have non-vanishing expectation values between eigenstates of the angular momentum operator while the pairing operator cannot but have zero expectation values between eigenstates of the number-of-particles operator. In this respect, the pairing degree of freedom is more similar to the octupole degree of freedom for which the expectation value between states having a definite parity necessarily vanishes.

<sup>††</sup> Most of the ideas of this section have been taken from lectures at the Niels Bohr Institute given by Professor A. Bohr during the winter term of 1968 and from ref. <sup>10</sup>).

in the quadrupole case. Therefore, by analogy with (2.11) we define a gauge transformation

$$\mathcal{G}(\phi) = e^{-i\mathcal{N}\phi}, \quad (2.11')$$

where  $\mathcal{N}$  is the number-of-particles operator. Under the gauge transformation, an operator changes according to the change in particle number associated with the operator. For instance, the one-particle creation operator and the operator  $P$  transform, respectively

$$\begin{aligned} c_v^{+'} &= \mathcal{G}(\phi)c_v^+ \mathcal{G}^{-1}(\phi) = e^{-i\phi} c_v^+, \\ P' &= \mathcal{G}(\phi)P \mathcal{G}^{-1}(\phi) = e^{-2i\phi} P. \end{aligned}$$

Therefore, the deformation parameters  $\alpha_\mu$  transform according to

$$\alpha'_{\pm 2} = \alpha_{\pm 2} e^{\mp 2i\phi}, \quad (2.9')$$

and the requirement that in the intrinsic system they are real

$$\text{Im}(\alpha'_2) = 0$$

implies that the gauge angle  $\phi$  is given by

$$\text{tg } 2\phi = i \frac{\alpha_2 - \alpha_{-2}}{\alpha_2 + \alpha_{-2}},$$

where the pairing deformation is measured by the absolute value  $\alpha$

$$\alpha = \alpha'_2 = (\alpha_2 \alpha_{-2})^{\frac{1}{2}}. \quad (2.7')$$

In the next two sections we construct the analogue of the Bohr collective Hamiltonian for the pairing case, in which the collective variables are the intrinsic parameter  $\alpha$  and the gauge angle  $\phi$ . By analogy with (2.10) the collective wave function is given by

$$\Psi_{n,A}(\alpha, \phi) = \frac{1}{\sqrt{2\pi}} \varphi_{n,A}(\alpha) e^{iA\phi} \quad (2.10')$$

which are characterized by the number of particles  $A$  and the quantum number  $n$  associated with the  $\alpha$  degree of freedom. Essentially, the same wave function was used by Ginsburg and Landau <sup>9)</sup> in describing superconductivity in solids. The nuclei described by the BCS wave function <sup>3)</sup> correspond to those that have a large stability with respect to a change in  $\alpha$  from the equilibrium position given by (2.6'). The low-energy collective states represent rotations in the angular variable  $\phi$  and therefore are associated in bands of states having essentially the same intrinsic function  $\varphi_{n,A}(\alpha) \approx \varphi_n(\alpha)$  but differing in the rotational term (for instance, the set of ground states of neighbouring even nuclei constitute one of these bands). Higher excitations are generated by vibrations of the system around the equilibrium shape (pairing vibrations in superconducting nuclei <sup>6)</sup>).

In normal nuclei, the energies associated with the two degrees of freedom  $\alpha$  and  $\phi$  are about equal and a phonon-like spectrum does appear.

### 3. Determination of the collective parameters

#### 3.1. POTENTIAL ENERGY SURFACE

The BCS solution

$$|\tilde{0}\rangle = \prod_{\nu} (U_{\nu} + V_{\nu} c_{\nu}^{\dagger} c_{\nu}^{\prime\dagger}) |0\rangle \quad (3.1)$$

is always an eigenfunction of the pairing field Hamiltonian (2.4') in the intrinsic system ( $\Delta'_2 = \Delta'_{-2} = \Delta$ , real) for any value of the potential deformation  $\Delta$  provided

$$\begin{aligned} U_{\nu} &= \frac{1}{\sqrt{2}} \left( 1 + \frac{e_{\nu} - \lambda}{E_{\nu}} \right)^{\frac{1}{2}}, \\ V_{\nu} &= \frac{1}{\sqrt{2}} \left( 1 - \frac{e_{\nu} - \lambda}{E_{\nu}} \right)^{\frac{1}{2}}, \end{aligned} \quad (3.2)$$

where  $E_{\nu} = [(e_{\nu} - \lambda)^2 + \Delta^2]^{\frac{1}{2}}$ . The potential energy is given by the expectation value of the two-body pairing Hamiltonian  $H_{s,p} + H_p$ . The pairing force contributes with a term

$$\langle \tilde{0} | H_p | \tilde{0} \rangle = -G\alpha^2 - G \sum_{\nu} V_{\nu}^4 \quad (3.3)$$

where

$$\alpha = \langle \tilde{0} | P | \tilde{0} \rangle = \sum_{\nu} U_{\nu} V_{\nu} = \frac{1}{2} \Delta \sum_{\nu > 0} \frac{1}{E_{\nu}}, \quad (3.3a)$$

(see also eqs. (2.5')). The second term in eq. (3.3) may be neglected because it is of the order of  $\Omega_t$  times  $\dagger$  smaller than the first one, where  $\Omega_t$  is the total degeneracy.

The total potential energy surface includes in addition to the term (3.3) a contribution from the single-particle potential, and therefore

$$V(\alpha) \equiv \langle \tilde{0} | H | \tilde{0} \rangle = \langle \tilde{0} | H_{s,p} | \tilde{0} \rangle + \langle \tilde{0} | H_p | \tilde{0} \rangle = 2 \sum_{\nu > 0} V_{\nu}^2 e_{\nu} - G\alpha^2. \quad (3.4)$$

In the interval  $0 \leq \alpha \leq 2\Omega_t$  this potential has only one minimum at the origin for  $G < G_c$ . There are two extreme values, a maximum at the origin and a minimum in the interval  $0 < \alpha < 2\Omega_t$ , if  $G > G_c$ . The position of this last extreme value is given by the BCS equation  $2/G = \sum_{\nu > 0} 1/E_{\nu}$ . The value  $G_c$  corresponds to the smallest value of  $G$  for which this equation has a solution. The BCS approximation assumes that the wave function has zero amplitude for  $\Delta$  away from this equilibrium position.

$\dagger$  We have checked this statement for  $\Omega = 100$  and  $\Omega = 20$  (see sect. 7) by comparing the results when the second term of eq. (3.3) was not included in the calculation of the potential energy. No significant differences appeared in the results.

As said before we are going to treat only the symmetric model. In this case there is a natural value of the Lagrange multiplier fixing the number of particles, namely the energy equidistant from levels above and below. In the following we shall take this energy to be the zero point of our energy scale ( $\lambda = 0$ ).

Further discussion on the asymptotic behaviour of the potential is done in sect. 5.

### 3.2. KINETIC ENERGY TERMS

The solution of the time-dependent Schrödinger equation

$$i\hbar \frac{\partial}{\partial t} |\psi(t)\rangle = H'_p |\psi(t)\rangle, \quad (3.4)$$

may be expressed as a linear combination of the “instantaneous” eigenfunctions of the Hamiltonian  $H'_p = H'_p(t)$  defined in eq. (2.4')

$$H'_p(t) |\omega(t)\rangle = \varepsilon_\omega(t) |\omega(t)\rangle, \quad (3.5)$$

at any fixed value of  $t$ . Therefore

$$|\psi(t)\rangle = \sum_{\omega > 0} a_\omega(t) |\omega(t)\rangle \exp \left[ -i \int_{t_0}^t \varepsilon_\omega(t') dt' / \hbar \right], \quad (3.6)$$

and eq. (3.4) is equivalent to the set of coupled differential equations

$$\dot{a}_\omega(t) = - \sum_{\nu > 0} a_\nu(t) \langle \omega(t) | \frac{\partial}{\partial t} | \nu(t) \rangle \exp \left[ i \int_{t_0}^t (\varepsilon_\omega(t') - \varepsilon_\nu(t')) dt' / \hbar \right]. \quad (3.7)$$

In order to solve eq. (3.7) by perturbation theory<sup>14</sup>), we begin assuming that the system spends most of its time in a particular state  $|\tilde{0}(t)\rangle$  (adiabatic approximation). For instance,  $|\tilde{0}(t)\rangle$  is the determinantal wave function obtained by filling the lowest single-particle levels, if we are treating the dilatation of a doubly magic nucleus. The determinantal state varies with time as the radius of the single-particle potential changes. In the present case  $|\tilde{0}(t)\rangle$  represents the BCS ground state and changes with time as the gap  $\Delta$  and the gauge angle  $\phi$  do. The states  $|\omega(t)\rangle$  which are connected to  $|\tilde{0}(t)\rangle$  by the time differential operator are two-quasiparticle states  $|\omega(t)\rangle = \alpha_\omega^+ \alpha_\omega^+ |\tilde{0}(t)\rangle$  with excitation energies  $\varepsilon_\omega - \varepsilon_0 = 2E_\omega$ . The assumption of adiabaticity can be rephrased by saying that the perturbative expansion of the coefficients

$$a_\nu(t) = a_\nu^{(0)}(t) + a_\nu^{(1)}(t) + a_\nu^{(2)}(t) + \dots, \quad (3.8)$$

is rapidly convergent,  $\langle \omega(t) | \partial / \partial t | \nu(t) \rangle$  being the expansion parameter and that

$$a_\nu^{(0)}(t) = \delta(\nu, 0). \quad (3.9)$$

Consequently

$$a_\omega^{(1)}(t) = - \int_{t_0}^t \langle \omega(t') | \frac{\partial}{\partial t} | \tilde{0}(t') \rangle \exp [i(\varepsilon_\omega(t') - \varepsilon_0(t')) t' / \hbar] dt'. \quad (3.10)$$

This integration can be simply performed in the adiabatic limit, in which the matrix elements  $\langle \omega(t) | \partial/\partial t | \tilde{0}(t) \rangle$  and the energies  $\varepsilon_\omega(t)$  change little during an amount of time of the order of the "intrinsic" periods  $\hbar/(\varepsilon_\omega - \varepsilon_0)$ . In such a case

$$a_\omega^{(1)}(t) = i\hbar \frac{\langle \omega(t) | \partial/\partial t | \tilde{0}(t) \rangle}{\varepsilon_\omega(t) - \varepsilon_0(t)} \exp [i(\varepsilon_\omega(t) - \varepsilon_0(t))/\hbar] + c, \quad (3.11)$$

where  $\langle \omega(t) | \partial/\partial t | \tilde{0}(t) \rangle$  and  $\varepsilon_\omega(t) - \varepsilon_0(t)$  are suitable time averages. Therefore, under the adiabatic hypothesis and requiring the wave function  $|\psi(t)\rangle$  to be normalized up to second order we obtain

$$|\psi(t)\rangle = \left\{ \left[ 1 - \frac{1}{2}\hbar^2 \sum_{\omega>0} \frac{|\langle \omega(t) | \partial/\partial t | \tilde{0}(t) \rangle|^2}{(\varepsilon_\omega(t) - \varepsilon_0(t))^2} \right] |\tilde{0}(t)\rangle + i\hbar \sum_{\omega>0} \frac{\langle \omega(t) | \partial/\partial t | \tilde{0}(t) \rangle}{\varepsilon_\omega(t) - \varepsilon_0(t)} |\omega(t)\rangle \right\} \times \exp [-i\varepsilon_0(t)t/\hbar], \quad (3.12)$$

or in other words,  $|\psi(t)\rangle$  is obtained in the base of eigenfunctions of  $H'(t)$  by treating the operator

$$H'' = -i\hbar \frac{\partial}{\partial t} \quad (3.13)$$

in ordinary Schrödinger perturbation theory. From now on the explicit dependence of the different magnitudes on  $t$  is not displayed any more. As is easily seen the wave function  $|\psi\rangle$  does not contain all the possible second-order terms. The missing ones are

$$\left\{ -\hbar^2 \sum_{\omega_1, \omega_2>0} \sum_{\nu>0} \frac{\langle \omega_1, \omega_2 | \partial/\partial t | \nu \rangle \langle \nu | \partial/\partial t | \tilde{0} \rangle}{(\varepsilon_{\omega_1\omega_2} - \varepsilon_0)(\varepsilon_\nu - \varepsilon_0)} |\omega_1 \omega_2\rangle \right. \\ - \hbar^2 \sum_{\nu>0} \sum_{\omega>0} \frac{\langle \omega | \partial/\partial t | \nu \rangle \langle \nu | \partial/\partial t | \tilde{0} \rangle}{(\varepsilon_\omega - \varepsilon_0)(\varepsilon_\nu - \varepsilon_0)} |\omega\rangle \\ \left. + \hbar^2 \sum_{\nu>0} \frac{\langle \nu | \partial/\partial t | \tilde{0} \rangle \langle \tilde{0} | \partial/\partial t | \tilde{0} \rangle}{(\varepsilon_\nu - \varepsilon_0)^2} |\nu\rangle \right\} e^{-i\varepsilon_0 t/\hbar}. \quad (3.14)$$

These terms, however, do not contribute up to second order to the kinetic energy when the standard cranking model prescription is used

$$T = \langle \psi | H'_p | \psi \rangle - \langle \tilde{0} | H'_p | \tilde{0} \rangle = \sum_{\omega>0} \frac{|\langle \omega | H'' | \tilde{0} \rangle|^2}{2E_\omega}. \quad (3.15)$$

The Hamiltonian  $H'_p$  is diagonal in the quasiparticle representation. According to eq. (3.13)  $H''$  is

$$H'' = -i\hbar\dot{\alpha} \frac{\partial}{\partial \alpha} - i\hbar\dot{\phi} \frac{\partial}{\partial \phi}. \quad (3.16)$$

We have seen before that the number-of-particles operator  $\mathcal{N} = \sum_{\nu>0} (c_{\nu}^{\prime\dagger} c_{\nu}^{\prime} + c_{\nu}^{\prime\dagger} c_{\nu}^{\prime})$  is the canonical conjugate variable to  $\phi$ , i.e.

$$-i\hbar \frac{\partial}{\partial \phi} = \hbar \mathcal{N}. \quad (3.17)$$

We can then write <sup>†</sup>

$$H'' = -i\hbar \dot{\alpha} \frac{\partial}{\partial \alpha} + \hbar \dot{\phi} \mathcal{N}. \quad (3.16a)$$

The commutation relation between the number operator and the gauge angle  $\phi$  is satisfied as well by the operator  $\mathcal{N} - \mathcal{N}_0$  where  $\mathcal{N}_0$  is a constant. It is convenient to choose  $\mathcal{N}_0$  as the number of particles filling the states below the Fermi level. In this way the lowest state of the collective spectrum has  $\phi \approx \langle \tilde{0} | \mathcal{N} - \mathcal{N}_0 | \tilde{0} \rangle / \mathcal{I} = 0$ . Therefore,  $H''$  has matrix elements

$$\begin{aligned} \langle \omega | H'' | \tilde{0} \rangle &= -i\hbar \dot{\alpha} \frac{(U_{\omega}^2 - V_{\omega}^2)/E_{\omega}}{\sum_{\nu>0} (U_{\nu}^2 - V_{\nu}^2)/E_{\nu}} + \dot{\phi} 2U_{\omega} V_{\omega}, \\ \langle \omega | H'' | \nu \rangle &= 2\hbar \dot{\phi} (U_{\nu}^2 - V_{\nu}^2) \delta(\nu, \omega), \\ \langle \tilde{0} | H'' | \tilde{0} \rangle &= 0. \end{aligned} \quad (3.18)$$

Because  $\alpha$  and  $\phi$  are real quantities by definition (see sect. 2), their time derivatives must also be real. Thus, the first term on the right-hand side of eq. (3.16a) is purely

<sup>†</sup> The same result can be obtained by applying the operator  $\partial/\partial\phi$  to the BCS ground state expressed in the lab system of coordinates

$$\mathcal{G}^{-1}(\phi) | \tilde{0} \rangle = \prod_{\omega>0} (U_{\omega} + e^{2i\phi} V_{\omega} c_{\omega}^{\prime\dagger} c_{\bar{\omega}}^{\prime\dagger}) | 0 \rangle.$$

The state generated in this way is equal to

$$\frac{\partial}{\partial \phi} \mathcal{G}^{-1}(\phi) | \tilde{0} \rangle = 2i \sum_{\nu>0} V_{\nu} e^{2i\phi} c_{\nu}^{\prime\dagger} c_{\bar{\nu}}^{\prime\dagger} \prod_{\omega \neq \nu} (U_{\omega} + V_{\omega} e^{2i\phi} c_{\omega}^{\prime\dagger} c_{\bar{\omega}}^{\prime\dagger}) | 0 \rangle.$$

The corresponding overlap with a two-quasiparticle state

$$\mathcal{G}^{-1}(\phi) | \nu \rangle = \mathcal{G}^{-1}(\phi) \alpha_{\nu}^{\prime\dagger} \alpha_{\bar{\nu}}^{\prime\dagger} | \tilde{0} \rangle = (-V_{\nu} + e^{2i\phi} U_{\nu} c_{\nu}^{\prime\dagger} c_{\bar{\nu}}^{\prime\dagger}) \prod_{\omega \neq \nu > 0} (U_{\omega} + e^{2i\phi} V_{\omega} c_{\omega}^{\prime\dagger} c_{\bar{\omega}}^{\prime\dagger}) | 0 \rangle,$$

is equal to

$$\langle \nu | \mathcal{G}(\phi) \frac{\partial}{\partial \phi} \mathcal{G}^{-1}(\phi) | 0 \rangle = 2i U_{\nu} V_{\nu} = i \langle \nu | \mathcal{N} | \tilde{0} \rangle.$$

This relation is identical to eq. (3.17).

imaginary while the second term is real and, therefore, there are no interference terms proportional to  $\dot{\alpha}\phi$  in the expression for the kinetic energy given by eq. (3.15):

$$\begin{aligned}
 T &= \frac{1}{2}B(\alpha)\dot{\alpha}^2 + \frac{1}{2}\mathcal{J}(\alpha)\phi^2 \\
 &= \frac{1}{2} \sum_{\omega>0} \frac{|\langle \omega | \hbar \partial / \partial \alpha | \tilde{0} \rangle|^2}{E_\omega} \dot{\alpha}^2 + \frac{1}{2} \sum_{\omega>0} \frac{|\langle \omega | \hbar \mathcal{N} | \tilde{0} \rangle|^2}{E_\omega} \phi^2 \\
 &= \frac{1}{2} \hbar^2 \frac{\sum_{\nu>0} (U_\nu^2 - V_\nu^2)^2 / E_\nu^3}{[\sum_{\nu>0} (U_\nu^2 - V_\nu^2)^2 / E_\nu]^2} \dot{\alpha}^2 + \frac{1}{2} \hbar^2 \sum_{\nu>0} 4 \frac{U_\nu^2 V_\nu^2}{E_\nu} \phi^2. \quad (3.19)
 \end{aligned}$$

In consequence, the mass parameters are given by

$$B(\alpha) = \frac{\hbar^2 \sum_{\nu>0} (U_\nu^2 - V_\nu^2)^2 / E_\nu^3}{[\sum_{\nu>0} (U_\nu^2 - V_\nu^2)^2 / E_\nu]^2}, \quad (3.20)$$

$$\mathcal{J}(\alpha) = 4\hbar^2 \sum_{\nu>0} \frac{U_\nu^2 V_\nu^2}{E_\nu}. \quad (3.21)$$

A possible objection to the previous estimate of  $\mathcal{J}(\alpha)$  and  $B(\alpha)$  arises from the fact that one is interested in the values of these parameters for a definite deformation  $\alpha$ . Now, the initial value of the wave function deformation is  $\alpha_0 = \langle \tilde{0} | \sum_{\nu>0} c_\nu^\dagger c_\nu^\dagger | \tilde{0} \rangle$  whether

$$\begin{aligned}
 \alpha' &\equiv \langle \psi | \sum_{\nu>0} c_\nu^\dagger c_\nu^\dagger | \psi \rangle \\
 &= \alpha_0 - 2\hbar^2 \sum_{\nu>0} \frac{|\langle \nu | \partial / \partial t | 0 \rangle|^2}{4E_\nu^2} U_\nu V_\nu \\
 &+ \hbar^2 \phi^2 \sum_{\nu>0} \frac{(U_\nu^2 - V_\nu^2)^2}{E_\nu^2} U_\nu V_\nu + \frac{i}{\sum_{\nu>0} e_\nu^2 / E_\nu^3} \hbar^2 \dot{\alpha} \phi \sum_{\nu>0} \frac{(U_\nu^2 - V_\nu^2)}{2E_\nu^3}. \quad (3.22)
 \end{aligned}$$

There appears then an uncertainty in the value of the deformation for which the mass parameters are determined. A second objection to eq. (3.15) is that one should use the expectation value of the total two-body Hamiltonian  $H = H_{s.p.} + H_p$  in order to obtain both the potential and kinetic contributions to the total energy, and not the field approximation Hamiltonian  $H'$ . Actually, the two above-mentioned objections, are closely related to each other (see below). In what follows, we present an alternative way of calculating the inertial parameters which is free of these objections and which gives the same expression (3.15).

It is shown that in the framework of the standard cranking model and at least for a symmetric system of levels the correct deformation to be taken is the one given by the wave function  $|\psi\rangle$  in the absence of velocity-dependent terms. We require that the

deformation  $\alpha$  of the system remains constant and equal to  $\alpha_0$  when cranking the wave function. To achieve this result, we allow the deformation of the potential to be a function of the velocities  $\dot{\alpha}$  and  $\dot{\phi}$ <sup>†</sup>. In this case we have to replace the BCS state  $|\tilde{0}\rangle$  in eq. (3.12) by

$$|\tilde{\sigma}'\rangle = |\tilde{\sigma}\rangle + \delta\Delta \frac{\partial}{\partial\Delta} |\tilde{\sigma}\rangle + \delta\lambda \frac{\partial}{\partial\lambda} |\tilde{\sigma}\rangle + \delta\phi \frac{\partial}{\partial\phi} |\tilde{\sigma}\rangle.$$

We then obtain

$$\langle\tilde{\sigma}'| \sum_{\nu>0} c_{\nu}^{\dagger} c_{\nu}^{\dagger} |\tilde{\sigma}'\rangle = \alpha_0 + \frac{1}{2}\delta\Delta g_1 - i\delta\phi \sum_{\omega>0} 2U_{\omega} V_{\omega}, \quad (3.23)$$

where

$$g_n = S_n - \Delta^2 S_{n+2}, \quad (3.24a)$$

$$S_n = \sum_{\nu>0} 1/E_{\nu}^n. \quad (3.24b)$$

The term proportional to  $\delta\lambda$  vanishes in the symmetric case as expected. Taking into account simultaneously the change of  $\alpha$  due to the presence of time dependent terms in  $|\psi\rangle$  and to the change in  $\Delta$  and  $\phi$  we get (see eqs. (3.22) and (3.24)),

$$\begin{aligned} \alpha' = \alpha_0 - \hbar^2 \sum_{\nu>0} \frac{|\langle\nu|\partial/\partial t|\tilde{0}\rangle|^2}{2E_{\nu}^2} U_{\nu} V_{\nu} + \hbar^2 \dot{\phi}^2 \sum_{\nu>0} \frac{(U_{\nu}^2 - V_{\nu}^2)}{4E_{\nu}^2} 4U_{\nu} V_{\nu} \\ + \frac{i}{g_1} \hbar^2 \dot{\alpha} \dot{\phi} \sum_{\nu>0} \frac{(U_{\nu}^2 - V_{\nu}^2)^2}{2E_{\nu}^3} + \frac{1}{2}\delta\Delta g_1 - i\delta\phi \sum_{\nu>0} 2U_{\nu} V_{\nu}. \end{aligned} \quad (3.26)$$

The requirement  $\alpha' = \alpha_0$  implies

$$\begin{aligned} \delta\Delta = \frac{\hbar^2}{g_1} \sum_{\omega>0} \frac{|\langle\omega|\partial/\partial t|\tilde{0}\rangle|^2}{E_{\omega}^2} V_{\omega} U_{\omega} - \frac{\hbar^2 \dot{\phi}^2}{g_1} \sum_{\omega>0} \frac{(U_{\omega}^2 - V_{\omega}^2)^2}{2E_{\omega}^2} 4U_{\omega} V_{\omega}, \\ \delta\phi = \left( \frac{\hbar^2 \dot{\alpha} \dot{\phi}}{g_1} \sum_{\nu>0} \frac{(U_{\nu}^2 - V_{\nu}^2)^2}{2E_{\nu}^3} \right) / \sum_{\nu>0} 2U_{\nu} V_{\nu}. \end{aligned} \quad (3.27)$$

The total energy  $\mathcal{E}_t$  can be separated into a velocity-dependent and velocity-independent term

$$\mathcal{E}_t = \langle\psi|H|\psi\rangle \equiv \langle\psi|H_{s.p.}|\psi\rangle + \langle\psi|H_p|\psi\rangle = T(\alpha, \dot{\alpha}, \dot{\phi}) + V(\alpha).$$

The expectation value of the pairing Hamiltonian yields (aside from small terms of the order of those already neglected in eq. (3.4))

$$\langle\psi|H_p|\psi\rangle = -G\alpha^2, \quad (3.28)$$

<sup>†</sup> This is a simple extension of the method which has been applied initially by Beliaev<sup>4)</sup> to deal with the pairing plus quadrupole model in constructing potential energy surfaces.

while we obtain from the expectation value of the single-particle Hamiltonian

$$\begin{aligned}
 \langle \psi | H_{s.p.} | \psi \rangle &= 2 \sum_{\omega > 0} e_{\omega} V_{\omega}^2 + \Delta \delta \Delta g_1 \\
 &+ \hbar^2 \sum_{\omega > 0} \frac{(U_{\omega}^2 - V_{\omega}^2)}{2E_{\omega}} |\langle \omega | \frac{\partial}{\partial t} | 0 \rangle|^2 + \hbar^2 \phi^2 \sum_{\omega > 0} \frac{8U_{\omega}^2 V_{\omega}^2}{2E_{\omega}} (U_{\omega}^2 - V_{\omega}^2)^2 \\
 &= 2 \sum_{\omega > 0} e_{\omega} V_{\omega}^2 + \hbar^2 \sum_{\omega > 0} \frac{|\langle \omega | \partial / \partial t | 0 \rangle|^2}{2E_{\omega}}. \tag{3.29}
 \end{aligned}$$

We recognize the potential energy  $V(\alpha)$  of eq. (3.23) to be the sum of the expectation value given in eq. (3.28) plus the velocity-independent term of eq. (3.29). The sum of these two terms gives back the result of eq. (3.3). The second term in eq. (3.29) represents the kinetic energy and is identical with expression (3.15).

In what follows we discuss some properties associated with the structure of the kinetic energy as given by eq. (3.19). It can be shown that the fact that the matrix elements of  $\partial/\partial\alpha$  and  $\mathcal{N}$  are real also implies that the kinetic energy is invariant under gauge transformations. To show this we will express  $T$  in terms of the wave function distortion parameters  $\alpha_{\pm 2}$  defined in eq. (2.5'). Because of the condition  $\alpha_2^* = \alpha_{-2}$  one can write

$$\alpha_{\pm 2} = \alpha e^{\pm 2i\phi}, \tag{3.30}$$

where  $\phi$  is the angle appearing in the transformation between the lab and intrinsic systems (see eq. (2.9')). It is clear from eq. (2.9') that the transformation  $\mathcal{G}(\phi)$  when applied to the magnitudes defined by eq. (3.30) gives a real number invariant under gauge transformations. By means of eq. (3.30) we can write

$$e^{4i\phi} = \alpha_2 / \alpha_{-2}. \tag{3.31}$$

By means of eqs. (2.7') and (3.31) we can calculate

$$\begin{aligned}
 \frac{\partial \alpha}{\partial \alpha_2} &= \frac{1}{2} e^{-2i\phi}, & \frac{\partial \alpha}{\partial \alpha_{-2}} &= \frac{1}{2} e^{2i\phi}, \\
 \frac{\partial \phi}{\partial \alpha_2} &= -\frac{i}{4\alpha} e^{-2i\phi}, & \frac{\partial \phi}{\partial \alpha_{-2}} &= \frac{i}{4\alpha} e^{2i\phi}, \tag{3.32}
 \end{aligned}$$

and therefore

$$\begin{aligned}
 H'' &= -i\hbar \frac{\partial}{\partial t} = -i\hbar \dot{\alpha}_2^2 \frac{\partial}{\partial \alpha_2} - i\hbar \dot{\alpha}_{-2} \frac{\partial}{\partial \alpha_{-2}} \\
 &= -\frac{1}{2} i \left\{ \dot{\alpha}_2 e^{-2i\phi} \hbar \left( \frac{\partial}{\partial \alpha} + \frac{\mathcal{N}}{2\alpha} \right) + \dot{\alpha}_{-2} e^{2i\phi} \hbar \left( \frac{\partial}{\partial \alpha} - \frac{\mathcal{N}}{2\alpha} \right) \right\} \\
 &= -\frac{1}{2} i \hbar \dot{\alpha}_2 e^{-2i\phi} \left( \frac{\partial}{\partial \alpha} + \frac{\mathcal{N}}{2\alpha} \right) - \frac{1}{2} i \hbar \dot{\alpha}_{-2} e^{2i\phi} \left( \frac{\partial}{\partial \alpha} - \frac{\mathcal{N}}{2\alpha} \right).
 \end{aligned}$$

Thus

$$|\langle \omega | H'' | \tilde{0} \rangle|^2 = \frac{1}{2} \dot{\alpha}_2 \ddot{\alpha}_{-2} \hbar^2 \left( |\langle \omega | \frac{\partial}{\partial \alpha} | \tilde{0} \rangle|^2 + \frac{|\langle \omega | \mathcal{N} | \tilde{0} \rangle|^2}{2\alpha} \right) + \frac{1}{4\alpha^2} (\dot{\alpha}_2^2 \alpha_{-2}^2 + \ddot{\alpha}_{-2}^2 \alpha_2^2) \hbar^2 \left( |\langle \omega | \frac{\partial}{\partial \alpha} | \tilde{0} \rangle|^2 - \frac{|\langle \omega | \mathcal{N} | \tilde{0} \rangle|^2}{2\alpha} \right), \quad (3.33)$$

which implies through eq. (3.15)

$$T = \frac{1}{4} \left( B(\alpha) + \frac{1}{4\alpha^2} \mathcal{J}(\alpha) \right) \dot{\alpha}_2 \ddot{\alpha}_2 + \frac{1}{8\alpha^2} \left( B(\alpha) - \frac{1}{4\alpha^2} \mathcal{J}(\alpha) \right) (\dot{\alpha}_2^2 \alpha_{-2}^2 + \ddot{\alpha}_{-2}^2 \alpha_2^2). \quad (3.34)$$

It is easy to check that

$$\dot{\alpha}_2 \ddot{\alpha}_{-2} = \dot{\alpha}^2 + 4\alpha^2 \dot{\phi}^2, \quad (3.35a)$$

$$\alpha_2^2 \dot{\alpha}_{-2}^2 + \alpha_{-2}^2 \dot{\alpha}_2^2 = 2\alpha^2 (\dot{\alpha}^2 - 4\alpha^2 \dot{\phi}^2) \quad (3.35b)$$

are the only gauge invariant magnitudes quadratic in the velocities  $\dot{\alpha}_{\pm 2}$  that can be constructed. A rather general condition that can be imposed on the coefficients of the partial differential equation (3.33) is that they are analytic functions of  $\alpha^2$ . This actually implies

$$\lim_{\alpha \rightarrow 0} \left( B(\alpha) - \frac{\mathcal{J}(\alpha)}{4\alpha^2} \right) = 0. \quad (3.36)$$

This requirement is automatically fulfilled by the mass parameters as calculated with the cranking model prescription eqs. (3.20) and (3.21), i.e.,

$$B(\alpha) \Big|_{\alpha=0} = \frac{\mathcal{J}(\alpha)}{4\alpha^2} \Big|_{\alpha=0} = \frac{\sum_{\nu>0} 1/E_\nu^3}{\sum_{\nu>0} 1/E_\nu^2} \Big|_{\alpha=0}. \quad (3.37)$$

The relation (3.37) is the only one existing between  $\mathcal{J}(\alpha)$  and  $B(\alpha)$ . It may be pointed out that (3.36) is equivalent to the relation <sup>13)</sup>  $\mathcal{J}_z/B_\nu = 4\gamma^2$  between the moment of inertia associated with rotations around the symmetry axis  $\mathcal{J}_z$  and the mass parameter  $B_\nu$ , associated with  $\gamma$ -vibrations in quadrupole axially symmetric deformed nuclei. For the quadrupole cases, the relation analogous to (3.36) holds not only at a point ( $\alpha = 0$ ) but on the whole axis  $\gamma = 0$ .

#### 4. The quantum-mechanical Hamiltonian

In the previous section we derived the classical Hamiltonian depending on the variables  $\alpha$ ,  $\phi$  and their time derivatives. Its form is in general (see eqs. (3.4) and (3.19))

$$H = T(a, \dot{a}) + V(a), \quad (4.1)$$

$$T = \frac{1}{2} \sum_{m,n} G_{mn}(a) \dot{a}_m \dot{a}_n,$$

where  $a_m$  are the collective variables. According to Pauli<sup>12,13</sup>, the quantum mechanical Hamiltonian is obtained by substituting for the kinetic energy  $T$  the operator

$$T = -\frac{1}{2} \sum_{m,n} |G|^{-\frac{1}{2}} \frac{\partial}{\partial a_m} |G|^{\frac{1}{2}} G^{mn} \frac{\partial}{\partial a_n}, \quad (4.2)$$

where  $G$  is the determinant of the matrix  $G_{mn}$  and  $G^{-1}$  is the inverse matrix. In our case,

$$G = \begin{pmatrix} B & 0 \\ 0 & \mathcal{J} \end{pmatrix}, \quad G^{-1} = \begin{pmatrix} 1/B & 0 \\ 0 & 1/\mathcal{J} \end{pmatrix}, \quad (4.3)$$

where the magnitudes  $\mathcal{J}$  and  $B$  are defined in eqs. (3.20) and (3.21).

The quantum mechanical kinetic energy is equal to

$$\begin{aligned} T &= \frac{1}{2} \frac{\hbar^2}{\sqrt{\mathcal{J}B}} \left\{ \frac{\partial}{\partial \phi} \sqrt{\frac{B}{\mathcal{J}}} \frac{\partial}{\partial \phi} + \frac{\partial}{\partial \alpha} \sqrt{\frac{\mathcal{J}}{B}} \frac{\partial}{\partial \alpha} \right\} \\ &= -\frac{\hbar^2}{2\mathcal{J}} \frac{\partial^2}{\partial \phi^2} - \frac{1}{2} \hbar^2 \left( \frac{1}{\mathcal{J}B} \frac{\partial \mathcal{J}}{\partial \alpha} - \frac{1}{B^2} \frac{\partial B}{\partial \alpha} \right) \frac{\partial}{\partial \alpha} - \frac{\hbar^2}{2B} \frac{\partial^2}{\partial \alpha^2}. \end{aligned} \quad (4.4)$$

Because (2.10') is an eigenfunction of the operator  $i\hbar \partial/\partial \phi$  with eigenvalue proportional to the number of particles, we can replace in eq. (4.4) the first term by

$$-\frac{1}{2\mathcal{J}} \frac{\partial^2}{\partial \phi^2} \rightarrow \frac{(A - \mathcal{N}_0)^2}{2\mathcal{J}}. \quad (4.5)$$

This is completely equivalent to the usual replacement that is done in the kinetic energy of a particle moving in an axially symmetric quadrupole deformed potential. The term (4.5) is thus a centrifugal term which, at least for small values of  $\alpha$  tends to increase the deformation of the system.

The volume element in the Pauli prescription is equal to

$$d\tau = |G|^{\frac{1}{2}} \prod_n da_n = \sqrt{\mathcal{J}B} d\alpha d\phi. \quad (4.6)$$

The form of this volume element is closely connected with the coefficients of the last two terms in eq. (4.4). This statement may be verified through the usual proof of orthogonality of the eigenfunctions

$$\begin{aligned} \int (\psi_1^* H \psi_2 - \psi_2^* H \psi_1) d\tau &= (E_2 - E_1) \int \psi_2^* \psi_1 d\tau \\ &= \frac{1}{2} \hbar^2 \int \psi_2^* \frac{\partial^2}{\partial \alpha^2} \psi_1 \sqrt{\frac{\mathcal{J}}{B}} d\alpha + \frac{1}{2} \hbar^2 \int \psi_1^* \frac{\partial^2}{\partial \alpha^2} \psi_2 \sqrt{\frac{\mathcal{J}}{B}} d\alpha \\ &\quad - \frac{1}{2} \hbar^2 \int \frac{1}{B\sqrt{\mathcal{J}B}} \left( B \frac{\partial \mathcal{J}}{\partial \alpha} - \mathcal{J} \frac{\partial B}{\partial \alpha} \right) \left[ \psi_2^* \frac{\partial}{\partial \alpha} \psi_1 - \psi_1^* \frac{\partial}{\partial \alpha} \psi_2 \right] d\alpha. \end{aligned}$$

Integrating by parts the first term on the right-hand side, and assuming that the wave functions vanish at the extreme values of  $\alpha$

$$\begin{aligned}
 (E_2 - E_1) \int \psi_2^* \psi_1 \, d\tau &= \frac{1}{2} \hbar^2 \int \left[ \frac{\partial}{\partial \alpha} \left( \psi_2^* \sqrt{\frac{\mathcal{J}}{B}} \right) \frac{\partial}{\partial \alpha} \psi_1 \, d\alpha + \frac{1}{2} \hbar^2 \int \psi_1^* \frac{\partial^2}{\partial \alpha^2} \psi_2 \sqrt{\frac{\mathcal{J}}{B}} \, d\alpha \right. \\
 &\quad \left. - \frac{1}{4} \hbar^2 \int \frac{1}{B \sqrt{\mathcal{J} B}} \left( B \frac{\partial \mathcal{J}}{\partial \alpha} - \mathcal{J} \frac{\partial B}{\partial \alpha} \right) \left[ \psi_2^* \frac{\partial}{\partial \alpha} \psi_1 - \psi_1^* \frac{\partial}{\partial \alpha} \psi_2 \right] \, d\alpha \right] \\
 &= \frac{1}{2} \hbar^2 \int \left[ \frac{\partial}{\partial \alpha} \sqrt{\frac{\mathcal{J}}{B}} - \frac{1}{2B \sqrt{\mathcal{J} B}} \left( B \frac{\partial \mathcal{J}}{\partial \alpha} - \mathcal{J} \frac{\partial B}{\partial \alpha} \right) \right] \left( \psi_2^* \frac{\partial}{\partial \alpha} \psi_1 - \psi_1^* \frac{\partial}{\partial \alpha} \psi_2 \right) \, d\alpha. \quad (4.7)
 \end{aligned}$$

The Schrödinger equation associated with the total Hamiltonian  $H$ , sum of the potential energy term (3.4) and of the kinetic energy term (4.4) is then

$$\left\{ -\frac{\hbar^2}{2B} \frac{\partial^2}{\partial \alpha^2} - \frac{1}{4} \hbar^2 \left( \frac{1}{\mathcal{J} B} \frac{\partial \mathcal{J}}{\partial \alpha} - \frac{1}{B^2} \frac{\partial B}{\partial \alpha} \right) \frac{\partial}{\partial \alpha} + \left( V(\alpha) + \frac{\hbar^2 M^2}{2\mathcal{J}} - \mathcal{E} \right) \right\} \varphi_{n, M}(\alpha) = 0, \quad (4.8)$$

where  $M = A - \mathcal{N}_0$ .

In the case in which  $\alpha_{\text{eq}} = 0$  and the zero point fluctuations are small<sup>†</sup>, we can approximate

$$\begin{aligned}
 V(\alpha) &= \frac{1}{2} V_0 \alpha^2 + V'_0, \\
 B(\alpha) &\equiv B_0 = \text{constant}, \\
 \mathcal{J}(\alpha) &= 4B_0 \alpha^2.
 \end{aligned} \quad (4.9)$$

Eq. (4.9) reads

$$-\frac{\hbar^2}{2B_0} \frac{\partial^2}{\partial \alpha^2} - \frac{1}{2B\alpha} \frac{\partial}{\partial \alpha} + \left( \frac{1}{2} V_0 \alpha^2 + \frac{M^2}{8B\alpha^2} - (\mathcal{E} - V'_0) \right) \varphi_{n, M}(\alpha) = 0, \quad (4.10)$$

which is the Schrödinger equation of the two-dimensional harmonic oscillator.

### 5. Asymptotic behaviour of the wave functions of the collective Hamiltonian

To solve numerically the pairing collective Hamiltonian we have made use of the variables  $\Delta$  and  $\phi$ . The corresponding differential eq. (4.8) reads

$$\left[ -h^{(2)}(\Delta) \frac{\partial^2}{\partial \Delta^2} - h^{(1)}(\Delta) \frac{\partial}{\partial \Delta} + h^{(0)}(\Delta) \right] \varphi_{n, M}(\Delta) = 0, \quad (5.1)$$

<sup>†</sup> The restoring force of the system has a positive contribution that comes from the single-particle Hamiltonian and a negative one proportional to  $G$ . For sufficiently small values of  $G$  we found the situation discussed above (harmonic limit).

where

$$h^{(0)}(\Delta) = -\mathcal{E}_M + V(\Delta) + \frac{M^2}{2\Delta^2 S_3}, \quad (5.2a)$$

$$h^{(1)}(\Delta) = \frac{2}{\Delta S_3} - \frac{\Delta S_5}{g_3 S_3} + \frac{5\Delta g_5}{g_3^2}, \quad (5.2b)$$

$$h^{(2)}(\Delta) = 2/g_3, \quad (5.2c)$$

$$V(\Delta) = g_{-1} - \frac{1}{4}G\Delta^2 S_1^2, \quad (5.2d)$$

where  $g_n$  and  $S_n$  are defined in eq. (3.24) and  $M$  in eq. (4.8). The lower and upper boundaries of the wave function deformation are  $\alpha_{\min} = 0$  and  $\alpha_{\max} = \frac{1}{2}\Omega_1$  respectively. The corresponding values of the potential deformation are  $\Delta_{\min} = 0$  and  $\Delta_{\max} = \infty$ . The corresponding volume element reads

$$d\tau = \frac{1}{2}\Delta\sqrt{g_3 S_3} d\Delta d\phi. \quad (5.3)$$

In table 1 we give the asymptotic values of the potential  $V(\Delta)$ . For  $G < G_c = 1/S_1(\Delta = 0)$  the potential has only one minimum located at  $\Delta = 0$  and the leading

TABLE 1

Asymptotic values of the pairing potential, the coefficients of the partial differential equation (5.1) and of the corresponding radial wave function  $\varphi_{n,m}$

	$\Delta \ll e_v$	$\Delta \gg e_v$
$V(\Delta)$	$\frac{1}{2}\Delta^2 S_1(1-G/G_c)$	$-\frac{1}{4}G\Omega^2 - \frac{1}{\Delta}$
$\partial V(\Delta)/\partial\Delta$	$\Delta(1-\frac{1}{2}GS_1)e(1)$	$\frac{1}{\Delta^2}e(-2)$
$\partial^2 V(\Delta)/\partial\Delta^2$	$(1-\frac{1}{2}GS_1)(e(1)-3\Delta^2 e(3)) + \frac{1}{2}\Delta^2 e(1)e(3)G$	$-\frac{2}{\Delta^3}e(-2)$
$h^{(0)}(\Delta)$	$\frac{M^2}{2e(3)}\frac{1}{\Delta^2} - e(-1) - \mathcal{E}$	$\frac{M^2}{2\Omega} \Delta - \frac{1}{4}G\Omega^2 - \mathcal{E}$
$h^{(1)}(\Delta)$	$2/e(3)\Delta$	$4\Delta^4/e(-2)$
$h^{(2)}(\Delta)$	$2/e(3)$	$2\Delta^5/e(-2)$
	$M = 0$ constant	$z^{\frac{1}{2}} J_{\frac{1}{2}}(\frac{1}{2}z^{\frac{1}{2}})$ $z = \frac{1}{\Delta} (\frac{1}{2}[\frac{1}{2}G\Omega + \mathcal{E} e(-2) ])^{\frac{1}{2}}$
$\varphi_{n,m}(\Delta)$	$M \neq 0$ $\Delta^{\frac{1}{2}M}$	$sh(z)$ $z = \left(\frac{M^2}{4\Omega} e(-2)\right)^{\frac{1}{2}} \frac{1}{\Delta}$

The magnitudes  $g_n$  and  $S_n$  are defined in eq. (3.24) and  $e(n) = \Sigma_v |e_v|^{-n}$ .

term for  $\Delta \ll e_v$  is proportional to  $\Delta^2$ . For  $G = G_c$  the restoring force is zero and consequently the potential increases as  $\Delta^4$ . For  $G > G_c$ ,  $V(\Delta)$  has a negative slope near

the origin and a minimum for  $S_1(\Delta) = 2/G$  (i.e. for  $\Delta = \Delta_{\text{eq}}$ ). In all cases  $V(\Delta)$  tends to  $-\frac{1}{4}G\Omega^2$  for  $\Delta \gg e_v$ .

We have also displayed in table 1 the asymptotic behaviour of the coefficients  $h_n(\Delta)$  of the partial differential equation (5.1) and of the corresponding radial wave function for the bound state case ( $\mathcal{E} < -\frac{1}{4}G\Omega^2$ ). Only the regular solution has been considered. The general solution of eq. (5.1) for  $M = 0$  are the Airy functions. We have chosen the particular combination of them that tend to zero for  $\Delta \gg e_v$ . The function  $J_{\frac{1}{3}}$  is the Bessel function of order  $\frac{1}{3}$ . The normalization condition for the wave function reads

$$\int \varphi_{n,M}^* \varphi_{n,M} d\tau = 1, \quad (5.4)$$

where  $d\tau$  is defined in eq. (5.3). Because of the structure of the volume element, any wave function which tends to a constant for  $\Delta \gg e_v$  would be an acceptable normalizable wave function. To restrict the set of solutions to wave functions which fulfill  $\varphi_{n,M}(\Delta = \infty) = 0$  appears consequently arbitrary.

## 6. Numerical method

The differential equation (4.8) can be written as

$$h^{(2)}(x)\varphi_{\mathcal{E}}''(x) + h^{(1)}(x)\varphi_{\mathcal{E}}'(x) - h^{(0)}(\mathcal{E}, x)\varphi_{\mathcal{E}}(x) = 0, \quad (6.1)$$

$\mathcal{E}$  being the eigenvalue. The procedure used to solve eq. (6.1) was to reduce it to finite differences, that is, by approximating  $\varphi(x)$  by the discrete sequence  $\varphi_m = \varphi(m\varepsilon)$ ,  $\varepsilon$  being the integration step chosen and  $m$  an integer number. Within this approximation

$$\varphi'(x) \approx \frac{\varphi(x + \frac{1}{2}\varepsilon) - \varphi(x - \frac{1}{2}\varepsilon)}{\varepsilon} \approx \frac{\varphi(x + \varepsilon) - \varphi(x - \varepsilon)}{2\varepsilon} = \frac{\varphi_{m+1} - \varphi_{m-1}}{2\varepsilon}, \quad (6.2)$$

$$\varphi''(x) \approx \frac{\varphi(x + \varepsilon) + \varphi(x - \varepsilon) - 2\varphi(x)}{\varepsilon^2} = \frac{\varphi_{m+1} + \varphi_{m-1} - 2\varphi_m}{\varepsilon^2}. \quad (6.3)$$

With the aid of eqs. (6.2) and (6.3), the differential equation can be cast in the form

$$\varphi_{m+1}(2h_m^{(2)} + \varepsilon h_m^{(1)}) - \varphi_m(4h_m^{(2)} + 2\varepsilon^2 h_m^{(0)}(\mathcal{E})) + \varphi_{m-1}(2h_m^{(2)} - \varepsilon h_m^{(1)}) = 0. \quad (6.4)$$

If any two consecutive values  $\varphi_k$  and  $\varphi_{k+1}$  are provided (which is equivalent to giving the value of the function and its derivative at a given point), then the full sequence  $\varphi_n$  can be constructed by an iterative process with the aid of eq. (6.1). The function thus obtained depends parametrically on  $\mathcal{E}$ . As in the case of better known potentials, the solution with increasing number of nodes corresponds to increasing values of  $\mathcal{E}$ . We discuss below different searching procedures for  $\mathcal{E}$  with the condition that  $\lim_{m \rightarrow \infty} \varphi(m\varepsilon) = 0$ . In our case we can distinguish between two different situations: (i) the depth of the potential ( $V_0$ ) is large compared to the energy of the lowest state and its

width ( $W$ ) is such that the mass parameter  $B$  changes smoothly inside it. These two features make the function  $\varphi(x)$  have a very large derivative in the absolute value once outside the well for small departures of the parameter  $\mathcal{E}$  from the eigenvalue  $\mathcal{E}_a$ . For  $\mathcal{E} = \mathcal{E}_a$  one needs to integrate many times up to the radius of the well ( $R$ , defined as  $V(R) = \frac{1}{2}V(\Delta = \infty)$ ) before the wave function tends to a constant (asymptotic behaviour). For instance in the case of the ground state of the system with  $M = 0$ ,  $\Omega = 100$  and for a value  $G = \frac{1}{2}G_c$  one needs to go up to a value of  $x \approx 20R$  before reaching the asymptotic region. In this case, starting at the origin with the

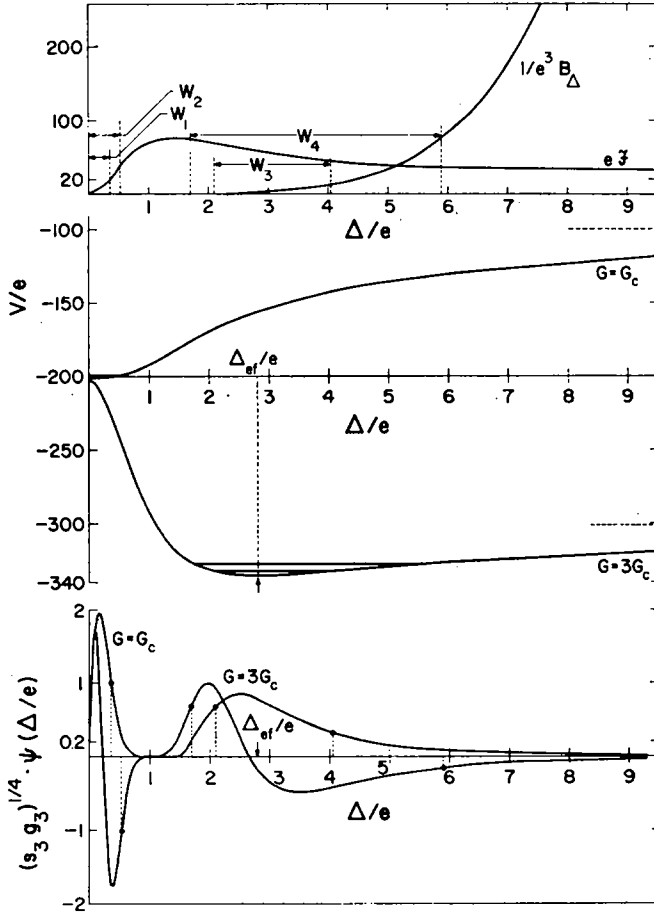


Fig. 1. The potential  $V(\Delta)$ , the inverse of the mass parameter  $B(\Delta)$  and the moment of inertia  $\mathcal{I}(\Delta)$  are plotted as a function of  $\Delta$  for the system  $\Omega = 100$ ,  $M = 0$  and for two values of the coupling constant  $G = G_c$  and  $G = 3G_c$ . The corresponding probability amplitudes of the two lowest states are also displayed. The quantities  $W_1$ ,  $W_2$  ( $W_3$ ,  $W_4$ ) are the widths of the well at the two lowest eigenvalues for  $G = G_c$  ( $G = 3G_c$ ).

For instance in the case of the ground state of the system with  $M = 0$ ,  $\Omega = 100$  and for a value  $G = \frac{1}{2}G_c$  one needs to go up to a value of  $x \approx 20R$  before reaching the asymptotic region. In this case, starting at the origin with the

proper  $x$ -dependence and checking both the number of nodes and the behaviour of  $\varphi'$ , a dicotomic procedure can be carried out and the eigenvalue can be determined with a prescribed precision. At each step, once the eigenvalue  $\mathcal{E}_n$  is obtained one can

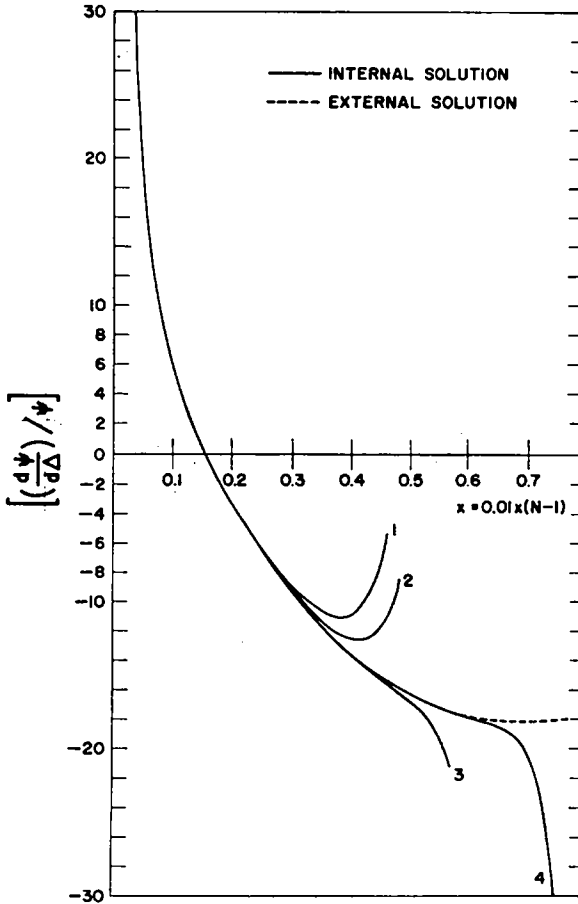


Fig. 2. The full line shows the logarithmic derivative of the internal solution corresponding to the system  $\Omega = 100$ ,  $M = 0$  and for a value of  $G = G_c$ . The solution of the partial differential equation (5.1) is obtained by method (i) (see sect. 6) after 6 (curve 1), 8 (curve 2), 12 (curve 3) and 20 (curve 4) iterations. The precision with which this eigenvalue is obtained is of the order of  $(\frac{1}{2})^n$ ,  $n$  being the number of iterations. No improvement is found however going beyond 12 iterations because the error due to the particular choice of the integration step ( $= 0.1$ ) will allow to get an accuracy of one part in  $10^4$ . The external solution is obtained by using any of the eigenvalues provided by the internal solution search. The differences are not possible to be plotted in the figure. The optimum matching point is  $x \approx 0.1$ .

start the integration at a point  $x = nR$  where  $n$  is a large number, and with the help of eq. (6.1) propagate it towards the origin. The internal and external solutions

are matched at the point in which the corresponding logarithmic derivatives have the same value (see fig. 2), (ii) the depth of the potential is such that the energy difference between the lowest eigenvalue to the asymptotic value ( $V_a \equiv V(\Delta = \infty)$ ) of the potential is small and the mass parameter  $B$  changes drastically over its range going from a finite value to zero. In this case the function  $\varphi$  has a very long decreasing tail even for values  $\mathcal{E} \neq \mathcal{E}_a$ . The procedure followed in this case is based on the fact that for  $\mathcal{E} = \mathcal{E}_a$ , the last node of  $\varphi_{\mathcal{E}}$  must be at infinity. Given a point  $x_0$ , two values  $\mathcal{E}_+$  and  $\mathcal{E}_-$  of the parameter  $\mathcal{E}$  can be found such that

$$\text{sign } \varphi_{\mathcal{E}_+}(x_0) \neq \text{sign } \varphi_{\mathcal{E}_-}(x_0) \quad (6.5)$$

and that  $\varphi_{\mathcal{E}_+}$  has the required number of nodes between  $x = 0$  and  $x = x_0$ . Under these circumstances  $\mathcal{E}_+ < \mathcal{E}_-$  and  $\text{sign } \{\varphi_{\mathcal{E}_+}(x)\} = (-1)^p$  where  $p =$  number of nodes, not including the one at the origin and the one at infinity. Interpolating between  $\mathcal{E}_+$  and  $\mathcal{E}_-$  a value  $\mathcal{E}_0$  can be found for which  $\varphi_{\mathcal{E}_0}(x_0) = 0$ . If  $x_0$  is increased by an amount  $\delta x$  a new value  $\mathcal{E}_1$  can be obtained by the same method such that  $\varphi_{\mathcal{E}_1}(x_0 + \delta x) = \varphi_{\mathcal{E}_1}(x_1) = 0$ . The sequence of numbers  $\{\mathcal{E}_k\}$  obtained through the condition

$$\varphi_{\mathcal{E}_k}(x_k) = 0, \quad x_k = x_0 + k\delta x, \quad (k = 1, 2, \dots) \quad (6.6)$$

tend to the eigenvalue  $\mathcal{E}_a$ . Numerically the searching process is stopped when two consecutive values  $\mathcal{E}_k$  and  $\mathcal{E}_{k+1}$  of the sequence  $\{\mathcal{E}_k\}$  differ in less than a prescribed value  $\eta$ . The sequence formed in this way is a monotonous one, that is, it is built by either upper or lower bounds of the eigenvalue. Stopping the calculation when  $|\mathcal{E}_{k+1} - \mathcal{E}_k| < \eta$  does not guarantee, in principle, that either of these two values will differ from the eigenvalue by the same amount (see for example, the sequence  $\psi_n = \sum_{k=1}^{k=n} 1/k$ ). In order to check this point we compare the convergence of the sequence  $\{\beta_k\} = \{|\mathcal{E}_k - \mathcal{E}_{k-1}|\}$  with the convergence of the sequences  $\{Ak^{-\alpha}\}$  and  $\{Ae^{-Ck}\}$ . In fig. 3 the sequence  $\{\beta_k\}$  is plotted as a function of  $k$  (for the ground state of the system  $\Omega = 100$ ,  $M = 0$ ,  $G = 3G_c$ ) together with the sequences  $\{Ak^{-1}\}$  and  $\{Ak^{-2}\}$ . The value of  $A$  was so chosen that all the sequences have the same value at  $k = 1$ . It is seen that  $\{\beta_k\}$  goes faster to zero than  $\{Ak^{-2}\}$  and in fact, from  $k_0 \approx 30$  on, it shows an exponential behaviour. We can then write

$$|\mathcal{E}_{k_0} - \mathcal{E}_a| \leq \sum_{k=0}^{\infty} |\mathcal{E}_k - \mathcal{E}_{k+1}| \approx \int_0^{\infty} Ae^{-Cx} dx = \frac{Ae^{-Ck_0}}{C}. \quad (6.7)$$

Therefore, if  $|\mathcal{E}_{k_0} - \mathcal{E}_{k_0+1}| \approx Ae^{-Ck_0} < \eta$  then  $|\mathcal{E}_{k_0} - \mathcal{E}_a| < \eta/C$ . Empirically, it was found that  $C$  is a constant of order unity.

In what follows we quote the empirically found range of validity of the two methods outlined above. For  $\Omega = 100$ , method (i) is valid up to  $G \approx 1.5 G_c$  (for  $M = 0$ ) and from there on method (ii) should be used. As  $\Omega$  is decreased the range of validity of the first method becomes smaller. For  $\Omega = 20$  ( $M = 0$ ) method (i) is valid up to  $G \approx 0.75 G_c$  whether for  $\Omega = 5$  ( $M = 0$ ) method (ii) should be used already for

$G \approx 0.25 G_c$ . This range of validity is determined basically by the behaviour of the mass that goes to zero more rapidly as a function of  $x$  with decreasing  $\Omega$ , leading to wave functions with very long tails and almost constant derivatives. A second fact that decides on the range of validity of method (i) is that for low  $\Omega$  values, the lowest level tends to be at a greater distance from the bottom of the well (see for example fig. 6), the wave function of this level has a lower barrier to penetrate. For some values of  $G$  close to the one that makes method (i) inapplicable, a hybridization of both methods was used.

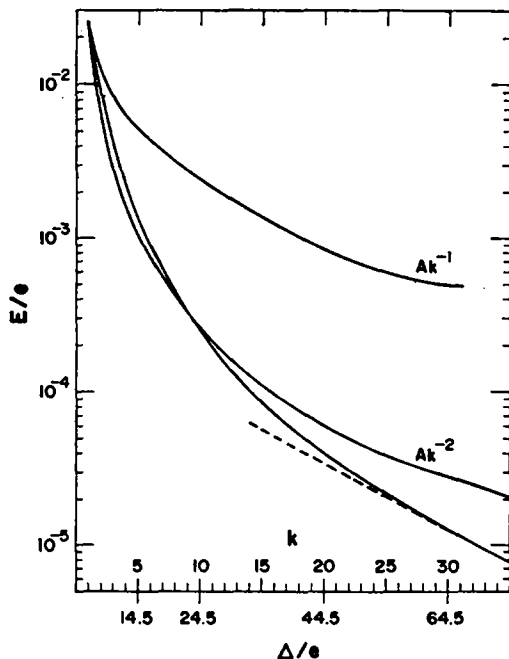


Fig. 3. The sequence of numbers  $\beta_k = |\epsilon_k - \epsilon_{k+1}|$  obtained as intermediate steps of the searching procedure (ii) for the case  $\Omega = 100$ ,  $G = G_c$  and  $M = 0$ , are displayed as a function of  $k$  (see text, sect. 6). Also displayed are the sequences of numbers  $Ak^{-1}$  and  $Ak^{-2}$ . It is seen that  $\{\beta_k\}$  tends faster to zero than any of these two sequences does and that for  $k \approx 30$  its decay is exponential.

Several checks on the numerical procedures were carried out. The integration routine was used to solve well-known differential equations of first and second order, obtained by setting for instance  $h^{(2)}(x) = \text{constant}$  and  $h^{(1)}x = 0$  or vice versa and  $h^{(0)}(x, \mathcal{E}) = \text{constant}$ . It was also used for solving the complete differential equation for the case  $G \ll G_c$ , in which case a nearly harmonic spectrum is found (see eq. (4.10) and corresponding discussion). Excellent agreement was found in all cases.

In using method (i) or (ii) a choice of the integration step must be made. Since all the structure of the wave function is found inside the well, the choice of the integration step must be made based on the width of the well at the eigenvalue. When

method (i) is applicable, a typical choice of 50 to 100 steps within the well will guarantee three decimal places in the eigenvalue and the orthonormality of the wave function check up to one part in  $10^4$ . As the well gets wider and shallower method (ii) should be used and one needs to go up to rather large values of  $x$  to obtain the desired accuracy. Typically one needs to go up to  $x = 15R$  to obtain a precision of  $10^{-4}$  in the eigenvalue. One can use in this case a larger integration step but in general, cumulative errors are then very important. One way to get around this problem is to perform an integration with variable step, increasing the step of integration as one goes further out in  $x$ , to regions in which the wave function has very little structure. The standard prescription used was to take the width of the well at a value 10 % above its minimum as a typical distance ( $R_0$ ), and to duplicate the step of integration at intervals equal to  $6 R_0$ .

### 7. Application of the solution to the two-level model

In the present section we test the collective solution of the pairing force Hamiltonian by comparing the results (henceforth, the collective results) with those obtained in an exact solution of the pairing-force problem (henceforth, the exact results).

We assume particles moving in two levels with identical pair-degeneracy  $\Omega$  separated by the distance  $D$ . In the symmetric case, we have therefore  $\mathcal{N}_0 = 2\Omega$ , the number of particles in the lowest collective state. Thus, the quantum number  $M$  in eq. (4.8) represents the difference

$$M = A - 2\Omega. \quad (7.1)$$

For the two-level model case, it is easier to solve exactly<sup>11,16)</sup> the pairing force problem, than to apply the collective approximation. In the representation characterized by the number of particles in the lowest and highest level, respectively, one has to diagonalize tridiagonal matrices.

In obtaining the exact results represented in figs. 4, 8 and 9, we have systematically subtracted a term  $GA$  from the exact energies. This term represents a self-energy, Hartree-type contribution of the pairing force and it is not supposed to be included in our treatment. The comparison between calculated and exact results is made first in the case of a very large degeneracy,  $\Omega = 100$ . In such a case we expect to minimize effects associated with the Pauli principle, at least if we treat a small number of particles or holes outside the closed shell ( $M = 0, 2$  and  $4$ ). We postpone the discussion of the effects due to large values of  $M$  and/or smaller values of  $\Omega$  to the second part of this section.

In the limit  $G \rightarrow \infty$ , the two-level model is equivalent to the one-level model. In this case, there is a simple expression for the energy of the ground states<sup>1,17)</sup>.

$$\mathcal{E}_M = -\frac{1}{4}GA(4\Omega - A + 2) + GA = -G\Omega^2 + \frac{1}{4}GM^2. \quad (7.2)$$

We thus see that the exact treatment predicts a rotational energy term  $\hbar^2 M^2 / 2\mathcal{I}$

with a moment of inertia  $\mathcal{I} = 2/G$  decreasing with increasing  $G$ . In the case of the solution corresponding to very stable superconducting systems, the collective Hamiltonian (4.8) yields a similar term. The value of the moment of inertia at equilibrium can be derived from (3.21).

$$\frac{\mathcal{I}^{eq}}{\hbar^2} = \lim \Delta^2 S_3 = \lim \left( S_1 - \sum_{\nu>0} \frac{e_\nu^2}{E_\nu^3} \right) = S_1 = \frac{2}{G}, \quad (7.3)$$

$$\Delta = \Delta_{eq} \gg |e_\nu|.$$

The left-hand side of fig. 4 reproduces the excitation energies of the  $M = 2$  and  $M = 4$  members of the ground state band.

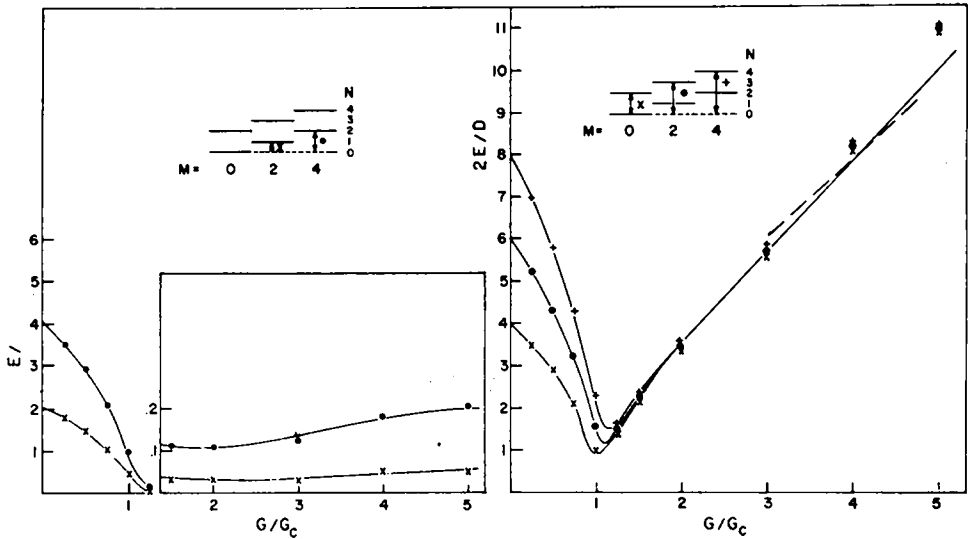


Fig. 4. The full lines represent the results of the exact calculation, while the crosses, dots, etc. correspond to the collective results. In each of the two sections of the figure, there is a level scheme clarifying which excitation energies are represented. In the level schemes, the states are characterized by the quantum numbers  $M$  and  $N$  where  $M$  is given in (7.1) and  $N$  is the number of phonons which the corresponding state would have as good quantum number if continued to the region  $G/G_c \ll 1$ . The left side of the figure represents excitation energies of the ground states of the systems with  $M = 2, 4$ . The right side represents the energies of the vibrational states corresponding to the  $M = 0, 2$  and  $4$  systems ( $\Omega = 100$ ). The dotted line indicates the two-quasiparticle energies  $2E_\nu = (\frac{1}{2}D^2 + \Delta^2_{eq})^{\frac{1}{2}} = G\Omega$ .

All energies are given in units of  $\frac{1}{2}D$  where  $D$  is the distance between the two levels.

The energies of these states in the vibrational limit ( $G/G_c$  very small) is given basically by the single-particle term, i.e.  $\mathcal{E}_2(\text{g.s.}) = D$  and  $\mathcal{E}_4(\text{g.s.}) = 2D$  (remember,  $\lambda = 0$ ). Here,  $\mathcal{E}_M(\text{g.s.})$  stands for the ground state energy of the system with  $M$  particles outside the closed shell. As  $G$  increases, the energy pattern should resemble the one given by eq. (7.2) as indicated by the fact that the collective moment of inertia coincides with the one level model prediction for superconductive nuclei (eq. (7.3)).

For  $G = \alpha G_c = \alpha D/2\Omega$  where  $\alpha$  is a number of order unity but greater than one,  $\mathcal{E}_2(\text{g.s.}) = G = \alpha D/2\Omega$  and  $\mathcal{E}_4(\text{g.s.}) = 4G = 4\alpha D/2\Omega$  (see eq. (7.2)). We see then that the ground state energies (measured from  $\mathcal{E}_0(\text{g.s.})$ ) decrease as a function of  $G$  typically from  $D$  to  $D/2\Omega$  and are of order  $G$  for  $G > G_c$ . It is a well-known result of the exact solution of the degenerate model that all other excitations are of order  $G\Omega$ . The numerical results show that  $|\mathcal{E}_2(\text{g.s.}) - \mathcal{E}_0(\text{g.s.})| \approx 10^{-5} \mathcal{E}_{M=0,2}(\text{g.s.})$ . The difference between the numerical and exact solutions are not representable in fig. 4 and are of order  $\lesssim 10^{-6} \mathcal{E}_{M=0,2}(\text{g.s.})$ . This is also the precision that we required in the numerical integration of the differential eq. (4.8). The agreement displayed in the figure constitutes therefore, evidence on the accuracy of the numerical method.

The ratio between the energies of the ground state levels is very approximately 4, already for values of  $G$  close (but larger) to  $G_c$ . For instance, the ratio has the value 3.93 for  $G = 1.5 G_c$ . Therefore, the rotational  $M^2$  law (analogous to the  $I(I+1)$  law for the quadrupole rotor) is very closely fulfilled even in cases where there are still significant deviations from the well-deformed coupling scheme. Therefore, the verification of the  $M^2$  law is not the most sensitive way of characterizing the presence of stable deformations. On the other hand, it is known<sup>16</sup>) that some matrix elements of the operator  $P$  {eq. (2.2')} have a dramatic dependence on  $G/G_c$ . These matrix elements are associated with two-nucleon reaction cross sections. We check below that the behaviour of these matrix elements allows one to decide the region of validity of the two pairing-coupling schemes (normal and superconductor). As usual, there is a transition region in which neither is applicable.

As is well known, the energies of the excited states differ by an amount  $\hbar\omega$  in the vibrational description of normal systems. From our results, we see that they become essentially degenerate for very deformed nuclei. This difference is due to the fact that the centrifugal term in eq. (4.8) is much more effective for small values of  $\Delta$ , because it diverges as  $1/\Delta^2$  in the limit  $\Delta \rightarrow 0$ .

The collective energies of the vibrational states depart from the exact values for  $G \geq 3G_c$ . This is to be expected since the vibrational motion is not adiabatic in well-deformed systems. The dotted line in fig. 4 represents the two-quasiparticle energy  $2(\frac{1}{4}D^2 + \Delta_{\text{eq}})^{\frac{1}{2}} = 2G\Omega$  (intrinsic excitations) and we see that the collective results deviate from the exact results from the point on which the intrinsic excitations become lower than the ones predicted on the basis of the adiabatic assumption.

The state representing a vibration around the deformed equilibrium position does not exist in the degenerate model, which is obtained in the limit  $G/G_c \rightarrow \infty$ , as previously mentioned. Correspondingly, in our calculation, the vibrational states become unbound for values of  $G/G_c \geq 6$ . More precisely, in order to find the first excited state once the ground state is found, the combination of methods (i) and (ii) (see previous section) is applied. For  $G \geq 6G_c$  and any value of  $M$ , the searching procedure is not able to find any suitable pair of eigenvalues, both of which are within the depth of the well.

In the case of vibrational states, the adiabatic model is supposed to have optimum

validity in the region of smallest excitation energies ( $G \approx G_c$ ). The model certainly improves over the unphysical results characteristic of the harmonic approximation (for instance, the result that the vibrational energy vanishes for  $G = G_c$ ). In the present treatment (and in the exact calculation) the zeros in the energies are replaced by

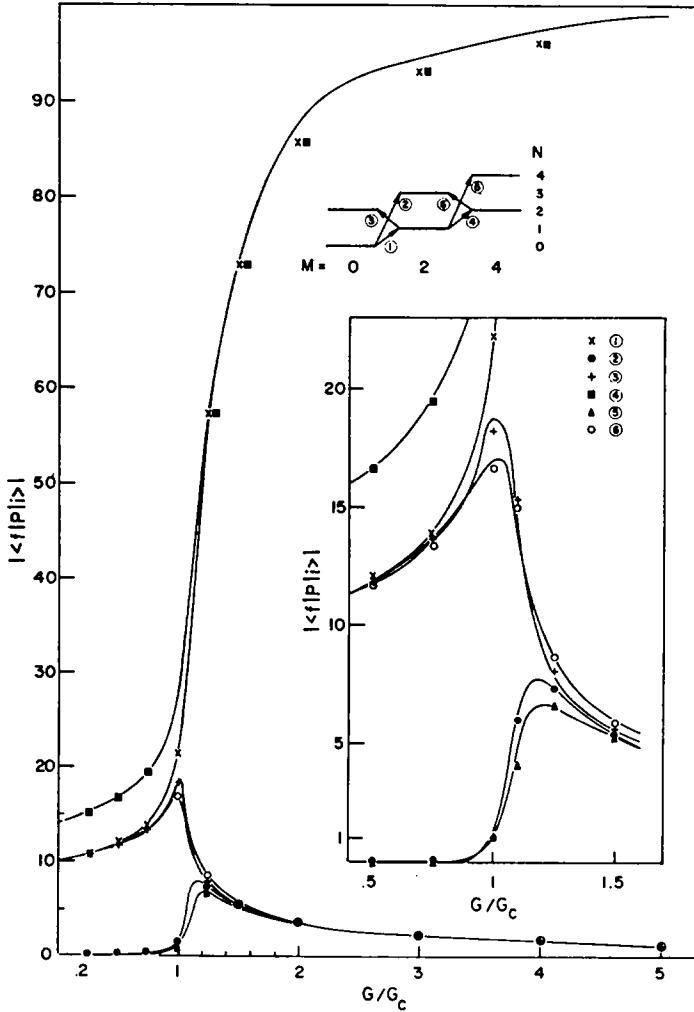


Fig. 5. The absolute value of the two-body transfer matrix element  $|\langle f|P|i\rangle|$  as a function of  $G/G_c$ , for the case  $\Omega = 100$ . The transition region  $G \approx G_c$  is displayed with an expanded scale at the right. See also the caption to fig. 4.

minima. In fig. 4, we see that these minima are somewhat pushed to the right of the point  $G = G_c$  (if  $|M| > 0$ ) as a consequence of centrifugal effects.

The matrix elements of the two-body transfer operator  $P$  may be divided into three groups:

a) Transitions within ground states. For small values of  $G$ , the ratio between the matrix elements of the transition between the ground states  $M = 0 \rightarrow 2$  and  $M = 2 \rightarrow 4$  is close to the number  $1/\sqrt{2}$ , characteristic of the vibrational scheme (fig. 5). Both transitions are systematically enhanced as  $G$  increases. Their rate of increase is particularly large in the region  $G \approx G_c$ , but they do not become infinite as the harmonic approximation predicts. Centrifugal effects are relatively small for  $G > G_c$  (see fig. 1) and, thus, both matrix elements ((1) and (4) in fig. 5) have essentially the same value for  $G \geq G_c$ . The matrix elements tend rather fast to their asymptotic value ( $\Omega$  in the present collective treatment or in the BCS solution,  $\Omega+1$  in the exact calculation).

The collective solution gives as expected, the same result as the BCS approximation for  $G/G_c \gg 1$ . In both cases one expects to find deviations of the order  $1/\Omega$  from the exact results.

b) Transitions between ground and vibrational states which are allowed in the vibrational coupling scheme (transitions (3) and (6) in fig. 5). Again the harmonic pattern is predicted in the case of small  $G$ : The corresponding matrix element increases in the same way as the ground state matrix element connecting the  $M = 0$  and  $M = 2$  systems, up to  $G/G_c \approx 1$ . For  $G/G_c \approx 1$  they present a maximum instead of the divergence predicted in the harmonic approximation. They become very small for stable superconducting nuclei. Therefore, the ratios between these transitions and the ground state transitions discussed in a) define whether we are dealing with a normal or a superconducting system<sup>16)</sup>.

c) Transitions between ground and vibrational states which are forbidden in the harmonic approximation (transitions (2) and (5) in fig. 5). Because for  $G > G_c$ , the levels populated by these transitions also become one-phonon states<sup>6)</sup> corresponding to vibrations around the deformed equilibrium position, their transition rates become equal to those of the previous group of levels (case 6) for stable superconductors. Therefore, since the transitions c) are suppressed in both extremes, a maximum at  $G \approx G_c$  is to be expected for them. This is indeed the case, and the presence of this maximum constitutes the most unambiguous way of characterizing transitional nuclei.

The previous observables are adequately reproduced by the collective model. On the contrary, we cannot hope to get accurate results concerning the energy of the  $M = 0$  lowest state. As it is remarked by Baranger and Kumar<sup>13)</sup>, the energy associated with the BCS solution represent the potential energy at equilibrium. Because the BCS wave function is obtained through a minimization procedure, any improvement on the solution should lead to a lower energy. On the contrary, the present collective approach adds to the BCS energy, the energy corresponding to the zero-point collective motion<sup>†</sup>.

<sup>†</sup> It is difficult however, to claim that one solution is better than the other on the basis of energy considerations alone and different physical properties should be chosen to make such kind of statements. For example, in the range  $1.5 \lesssim G/G_c \lesssim \infty$ , the energy of the ground state is given better by the BCS solution than by the collective solution. On the other hand, in the same range of  $G/G_c$ , the transitions of type a) are better reproduced by using the collective wave functions than the BCS solution (especially in the case of  $\Omega = 20$ ).

Another problem connected with the lowest collective state (and with all ground states) is the very existence of a solution. We have seen that the vibrational levels disappear for  $G \gg G_c$ . Does the same thing happen within our formalism to the ground state band? Fig. 6 represents the ratio between the energy of the zero-point motion of the lowest collective state and the depth of the potential well (difference between the values of the potential at  $\Delta \rightarrow \infty$  and at  $\Delta = \Delta_{eq}$ ). According to fig. 6, this ratio may tend to one for large values of  $G$ . In order that our model makes sense, it is imperative that such a convergence should occur, because the ground state band

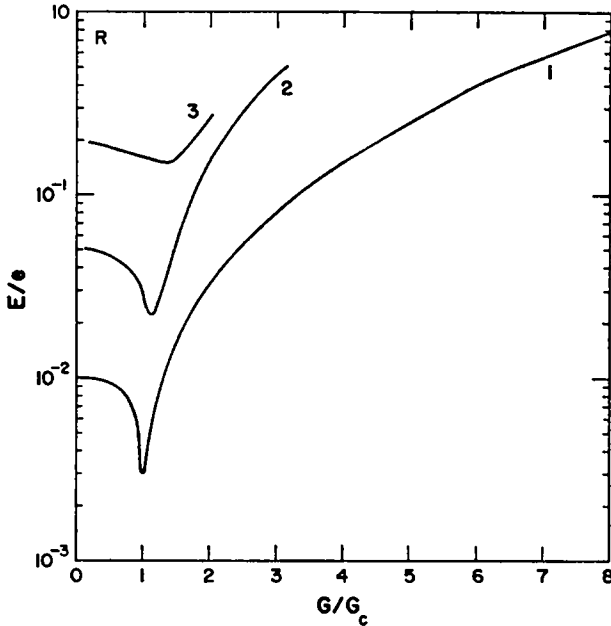


Fig. 6. The ratio between the zero-point energy of the collective motion and the depth of the potential well. Curves (1), (2) and (3) correspond to  $\Omega = 100$ , 20 and 5, respectively.

is always adiabatic and, indeed, it becomes even more adiabatic the larger the values of  $G$ . However, the convergence is difficult to verify numerically, since our method of integration of the differential equation loses precision when the wave function becomes very extended, because each step in the integration also becomes too large. In any case, the region in which we are able to find a solution extends considerably into the region in which the superfluid solution is valid, and we are able to reproduce accurately the exact results.

Let us now discuss the results of the calculation for larger values of  $M$ .

(i) If  $G \leq G_c$  a transition to the deformed coupling scheme may take place for a certain value of  $M$ . Strictly speaking, if  $M \neq 0$ , the centrifugal term  $\hbar^2 M^2 / 2\mathcal{J}$  represents a potential barrier for  $\Delta \rightarrow 0$ , and in consequence, the wave function vanishes at the origin (this is analogous to the familiar situation of a particle bound in a

spherically symmetric potential well and carrying an orbital angular momentum  $l \neq 0$ ). Although the wave function may be zero at the origin, that does not necessarily imply that the system has a permanent distortion. As  $M$  increases, the maximum of the wave function (or better of the probability amplitude) is pushed away from the origin. When the width of this peak becomes appreciably smaller than the value  $\Delta_m$  at which the maximum takes place, the system has gained energy by acquiring a permanent distortion stabilized around  $\Delta_m \approx \Delta_{eq}$ .

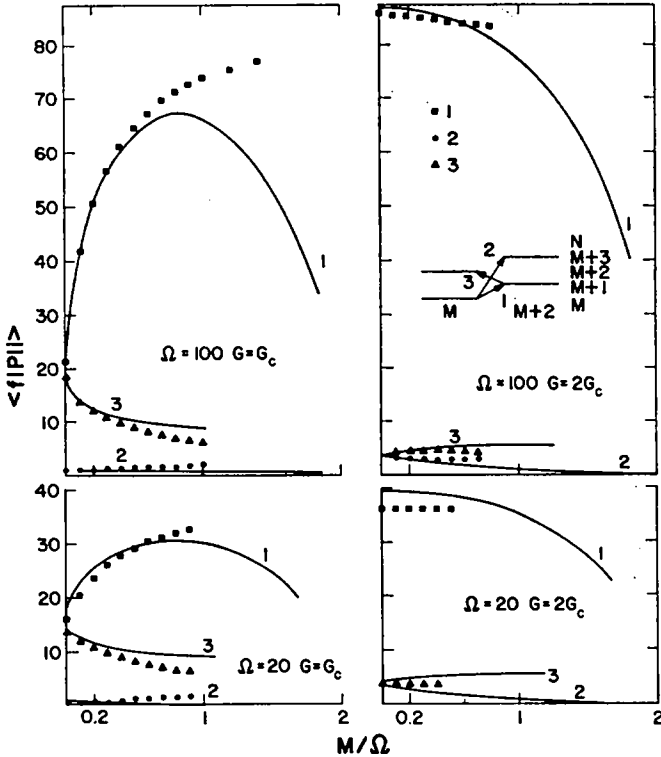


Fig. 7. The transition matrix elements for  $G = G_c$  and  $G = 2 G_c$  ( $\Omega = 100$  and  $\Omega = 20$ ) as a function of  $M/\Omega$ . The values corresponding to  $\Omega = 20$  are multiplied by the factor  $[(\Omega = 100)/(\Omega = 20)]^{\frac{1}{2}} = \sqrt{5}$  in order that the transition rates have the same values in the vibrational limit.

The results of fig. 7 support the idea of a gradual transition to the deformed coupling scheme, both in the case of  $\Omega = 100$  and  $\Omega = 20$  ( $G = G_c$ ). The transition rate between the ground states increases as a function of  $M$  and tend to the asymptotic values given in figs. 5 and 10. Simultaneously, the transition between the  $M+2$  ground and  $M$  first excited state (which is allowed in the vibrational model) decreases in intensity and tends towards the value of the transition between the  $M$  ground and the  $M+2$  first excited state (forbidden in the vibrational model). In fact, the curves of

fig. 7 ( $G = G_c$ ) are (as a function of  $M$ ) similar to the curves displayed in fig. 5 and 10 (as a function of  $G/G_c$ ). However, the phase transition is more dramatically displayed by the system with a fixed number of particles when  $G/G_c$  goes through 1.

(ii) We have seen that in the limit of very stable superconducting nuclei, the energies of the ground state band obey the  $M^2$  law. Therefore, in order to find whether the centrifugal term has produced a phase transition, we may calculate the ratio  $R_M = (\mathcal{E}_{M+4} - \mathcal{E}_M)/(\mathcal{E}_{M+2} - \mathcal{E}_M)$  for different values of  $M$ . This ratio has the value  $R_M^{(d)} = 2(M+2)/(M+1)$  in well-deformed cases. In table 2 we give several values of the ratio  $R_M/R_M^{(d)}$  for the case  $G = G_c$ . We see that the ratio increases rapidly with  $M$  for small values of  $M/\Omega$ . After a certain transition point the ratio is greater than, for instance, 0.9 and from there on it tends slowly to the asymptotic value 1.

TABLE 2

The ratio  $R_M = (\mathcal{E}_{M+4} - \mathcal{E}_M)/(\mathcal{E}_{M+2} - \mathcal{E}_M)$  between the energies of the system with  $M+4$  and  $M+2$  particles as measured from the energy of the system with  $M$  particles giving a measure of the degree of pairing distortion of the system

$\Omega = 100$	$M/\Omega$	0.	0.02	0.04	0.08	0.12	0.16	0.30	0.50
$R_M/R_M^{(d)}$	exact	0.555	0.806	0.880	0.934	0.955	0.966	0.984	0.990
	collective	0.545	0.798	0.876	0.934	0.955	0.966	0.984	0.990
$\Omega = 20$	$M/\Omega$	0	0.10	0.10	0.30	0.40	0.50		
$R_M/R_M^{(d)}$	exact	0.578	0.827	0.827	0.930	0.947	0.962		
	collective	0.563	0.873	0.903	0.939	0.959	0.972		

For the normal system  $R_M^{(n)} = 2$ , while for distorted systems  $R_M^{(d)} = 2(M+2)/(M+1)$ . We display the ratio  $R_M^{(c)}/R_M^{(d)}$  as a function of  $(M/\Omega)$  for the case of  $\Omega = 100$  and  $\Omega = 20$  and  $G = G_c$ .

(iii) We have seen that for very stable superconducting systems and small values of  $M/\Omega$ , the vibrational states become unbound for sufficiently large values of  $G$ . A similar behaviour takes place if we keep  $G$  fixed and we increase  $M$ . The vibrational state becomes unbound at  $M/\Omega = 1$ , if  $G = G_c$ , and at  $M/\Omega = 0.8$  if  $G = 2G_c$ .

(iv) Our collective adiabatic treatment must cease to be valid for some value of the ratio  $M/\Omega$ . In other words, the velocities  $\dot{\phi} = \hbar M/\mathcal{I}$  may eventually become so large that the assumption of adiabaticity cannot be maintained any longer. Fig. 7 indicates that the collective results are close to the exact results for  $|M/\Omega| \lesssim 1$ , but after the second level is half filled the results depart from each other to a large extent.

We have also performed calculations similar to those of the  $\Omega = 100$  case, for the degeneracies  $\Omega = 20$  and  $\Omega = 5$ .

The curves corresponding to  $\Omega = 20$  behave like those already shown for  $\Omega = 100$ , although the differences between the collective and exact results can now be represented in figs. 8 and 10. However, because these differences are small, the agreement can still be considered very good. Thus, all the previous discussion for  $\Omega = 100$  may be re-

peated in the case  $\Omega = 20$ . There are, nevertheless, some quantitative changes: the vibrational states become unbound for  $G \gtrsim 2.5 G_c$  (instead of  $G \gtrsim 6 G_c$ ) and the numerical solution presents convergence problems for the ground states if  $G \gtrsim 3 G_c$  (instead of  $G \gtrsim 8 G_c$ ). In fig. 7 and table 2 we display the results for  $\Omega = 20$  as a function of  $M$ . The collective solution agrees with the exact calculation again until  $|M/\Omega| \approx 1$ . The vibrational states become unbound for values of  $|M/G| = 0.9$  if  $G = G_c$  and  $|M/\Omega| = 0.5$  if  $G = 2G_c$ . These values are smaller than the corresponding numbers in the  $\Omega = 100$  case.

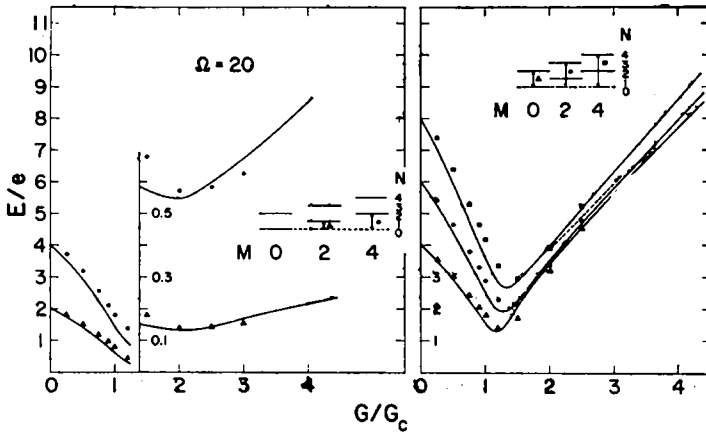


Fig. 8. Same caption as for fig. 4 but  $\Omega = 20$ .

Finally, we have studied the cases  $M = 0, 2, 4$  for the degeneracy  $\Omega = 5$ . The vibrational state for  $M = 2, 4$  are always unbound. In the case of  $M = 0$ , the vibrational state becomes unbound for  $G \geq 1.2 G_c$ . For this same value of  $G$ , convergence problems appear in the solution of the ground state corresponding to the  $M = 4$  system. The solution corresponding to  $M = 2$  (ground state) is obtained until  $G = 1.6 G_c$ . In general, the exact results are not very satisfactorily reproduced by the collective treatment (figs. 9 and 10) and therefore we are reminded that the language associated with the collective variables may be used only in a qualitative way for small degeneracies.

## 8. Conclusions

The significant part of this paper was not to provide another method for solving the pairing force problem:† On the contrary, our aim has been to contribute to the clarification of alternative descriptions of collective states in terms of the single-particle excitations and of collective variables.

† For a list of such methods, see ref. 1).

From the systematic agreement in the results displayed in the figures we can conclude that the present version of the collective treatment is adequate. In particular, the validity of some doubtful points in the model may be considered to be confirmed because of this agreement. These points are: a) the solution of a quantum mechanical problem through a detour involving semi-classical approximations (cranking model);

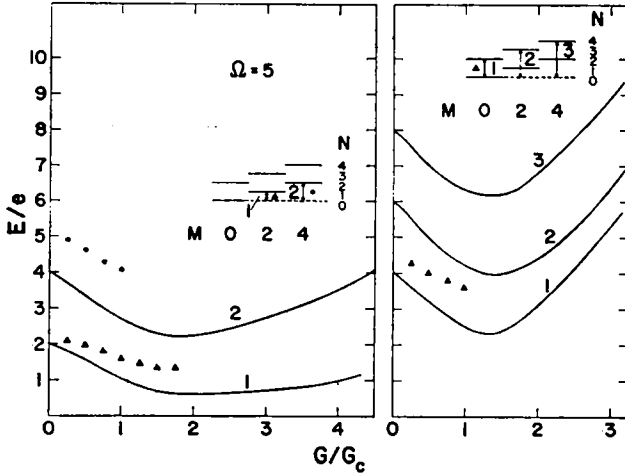


Fig. 9. Same caption as for fig. 4 but  $\Omega = 5$ .

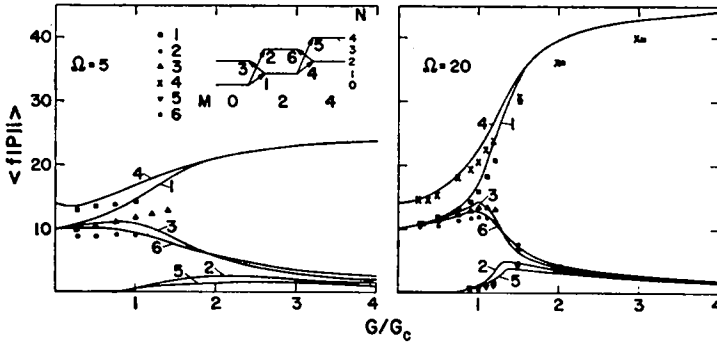


Fig. 10. Same caption as for fig. 5. The left side corresponds to  $\Omega = 5$  while the right side corresponds to  $\Omega = 20$ .

b) the boundary condition  $\psi(\Delta = \infty) = 0$ , which is not required as usually by the normalization condition; c) the fact that the probability density (see i.e. fig. 1) does not appear to be sufficiently peaked at a fixed value of  $\Delta$  ( $\approx \Delta_{eq}$ ) for large values of  $G$  in order to ensure the validity of the BCS solution (no fluctuations around  $\Delta_{eq}$ ). In spite of the width of the peak, (fig. 1) the results of the BCS solution are reproduced completely for values of  $G \gtrsim 3 G_c$ .

By means of the collective description of the pairing degree of freedom, we can treat in the same scheme, both normal and superfluid systems, avoiding the change of representation needed in the microscopic description <sup>6</sup>). Also intermediate situations ( $G/G_c \approx 1$ ) can be handled without any special difficulty in the present treatment of the pairing Hamiltonian.

Discussions with Professors Benjamin Bayman, Aage Bohr and Ben Mottelson are gratefully acknowledged.

### References

- 1) D. R. Bès and R. Sorensen, *Advances in nuclear physics*, Vol. 2 (Plenum Press, 1969) p. 129
- 2) A. Bohr, B. R. Mottelson and D. Pines, *Phys. Rev.* **110** (1958) 936
- 3) J. Bardeen, L. N. Cooper and J. R. Schrieffer, *Phys. Rev.* **108** (1957) 1175
- 4) S. T. Beliaev, *Mat. Fys. Medd. Dan. Vid. Selsk.* **31**, no. 11 (1959)
- 5) A. Bohr, *Compt. Rend. du Cong. Int. de physique nucléaire*, Paris 1969, Ed. Centre National de la Recherche Scientifique (Paris 1964) p. 487
- 6) D. R. Bès and R. A. Broglia, *Nucl. Phys.* **80** (1966) 289
- 7) O. Nathan, *Int. Symp. on nuclear structure* (Dubna, USSR, July 1968)
- 8) B. Sørensen, *Nucl. Phys.* **A97** (1967) 1
- 9) V. L. Ginsburg and L. D. Landau, *ZhETF (USSR)* **20** (1950) 1064;  
R. P. Feynman, R. B. Leighton and M. Sands, *The Feynman lectures on physics*, Vol. 1 (Addison Wesley, Massachusetts)
- 10) A. Bohr, *Int. Symp. on nuclear structure* (Dubna, USSR, July 1968)
- 11) J. Hogaasen-Feldman, *Nucl. Phys.* **28** (1961) 258
- 12) A. Bohr, *Mat. Fys. Medd. Dan. Vid. Selsk.* **26**, no. 14 (1952)
- 13) M. Baranger and K. Kumar, *Nucl. Phys.* **92** (1967) 608; **A110** (1968) 490, 529; **A122** (1969) 241
- 14) L. I. Schiff, *Quantum mechanics* (McGraw-Hill Book Co., New York, 1969) p. 207
- 15) W. Pauli, *Handbuch der Phys.* Vol. 24 (Springer, Berlin 1933) p. 120
- 16) R. A. Broglia, C. Riedel and B. Sørensen, *Nucl. Phys.* **A107** (1968) 1
- 17) B. R. Mottelson, *Cours de l'École d'Été de Physique Théorique des Houches 1958* (Dunoud, Paris, 1959)
- 18) B. Sørensen, *Nucl. Phys.* **A134** (1969) 1